Title: **Discovery of novel thrips vector proteins that bind to the plant bunyavirus, tomato spotted wilt virus.**

Short title (70 Characters): Identification of thrips proteins that interact with TSWV

Authors and affiliations:

Ismael E. Badillo-Vargas[#1], Yuting Chen[#2], Kathleen M. Martin[2], Dorith Rotenberg[2*], and Anna E. Whitfield[2*]

[1]Department of Entomology, Texas A&M AgriLife Research, Weslaco, Texas, United States of America

[2]Department of Entomology and Plant Pathology, North Carolina State University, Raleigh, North Carolina, United States of America

#IEBV and YC are joint first authors and contributed equally to this work.

*corresponding authors

E-mail: awhitfi@ncsu.edu, drotenb@ncsu.edu

Abstract

The plant-pathogenic virus, tomato spotted wilt virus (TSWV), encodes a structural glycoprotein (G_N) that, like with other bunyavirus/vector interactions, serves a role in viral attachment and possibly entry into arthropod vector host cells. It is well documented that *Frankliniella occidentalis* is one of seven competent thrips vectors of TSWV transmission to

plant hosts, however, the insect molecules that interact with viral proteins, such as G_N, during infection and dissemination in thrips vector tissues are unknown. The goals of this project were to identify TSWV-interacting proteins (TIPs) that interact directly with TSWV G_N and other structural proteins and to localize expression of these proteins in relation to virus in thrips tissues of principle importance along the route of dissemination. We report here the identification of six TIPs from first instar larvae (L1), the most acquisition-efficient developmental stage of the thrips vector. The TIPs were annotated and confirmed to interact with TSWV proteins, including G_N and the nucleocapsid (N) protein. Sequence analyses of these TIPs revealed homology to proteins associated with the infection cycle of other vector-borne viruses. Immunolocalization of the TIPs in L1s revealed robust expression in the midgut and salivary glands of *F. occidentalis*, the tissues most important during virus infection, replication and plant-inoculation. One of the TIPs, an endocuticular structural glycoprotein that bound G_N, co-localized with TSWV at the anterior region of the L1 midgut by 24 hours after ingestion of virus-infected plant tissue. These novel discoveries are essential for better understanding the interaction between persistent propagative plant viruses and their vectors, as well as for developing new strategies of insect pest management and virus resistance in plants.

Author Summary

Arthropod vectors play an essential role in the dissemination of viruses that cause diseases in humans, animals, and plants. More than 70% of viruses infecting plants and 40% of viruses infecting mammals are transmitted from one host to another by arthropod vectors. For negative-sense RNA viruses, the arthropod serves as a host as well by supporting virus replication in specific tissues and organs of the vector. The goal of this work was to identify vector/host proteins that bind directly to viral structural proteins and thus may play a role in

the infection cycle in the insect. Using the model plant bunyavirus, tomato spotted wilt virus (TSWV), and the most efficient thrips vector, we identified and validated six TSWV-interacting proteins from *Frankliniella occidentalis* first instar larvae. One protein, an endocuticle structural glycoprotein, was able to interact directly with the TSWV attachment protein, G_N. These proteins co-localized in infected insect cells, and we found a unique region of the thrips protein that bind to G_N. The TSWV-interacting proteins provide new targets for disrupting the virus-vector interaction and could be putative determinants of vector competence.

Introduction

Vector-borne diseases caused by animal- and plant-infecting viruses are some of the most important medical, veterinary, and agricultural problems worldwide [1, 2]. The majority of viruses infecting plants and animals are transmitted by arthropods. Understanding the viral and arthropod determinants of vector competence is important for basic knowledge of virus-vector interactions and development of new interdiction strategies to control disease. Significant progress has been made towards identification of virus determinants of transmission, but the interacting partners in vectors remain largely elusive. For negative-sense RNA viruses, vector/host factors that mediate the transmission process have not been well characterized.

Bunyavirales is the largest order of negative-sense RNA viruses; nine families are described (http://www.ictvonline.org/virustaxonomy.asp). The family *Tospoviridae* contains plant and insect-vector-infecting viruses that make up the genus *Orthotospovirus* [3-5]. Within this genus, there are eleven species and more than fifteen unassigned viruses that most likely will be classified as unequivocal members of the *Orthotospovirus* genus. *Tomato spotted wilt virus* (TSWV) is the model species within this genus and has been best

characterized in terms of viral host range, genome organization and protein functions [6, 7].

TSWV infects both monocotyledonous and dicotyledonous plants encompassing more than 1,000 plant species worldwide [8]. Due to the extremely wide host range, TSWV has caused severe economic losses to various agricultural, vegetable and ornamental crops. The TSWV virion has a double-layered, host-derived membrane studded with two glycoproteins (G_N and G_C) on the surface. The viral glycoproteins play an essential role in attachment to the thrips gut and fusion of the virus and host membranes [7, 9-11]. Virus particles range in size from 80 to 120 nm in diameter, and inside the particle are three genomic RNAs designated long (L), medium (M) and small (S) RNA based on the relative size of each molecule. The L RNA is negative sense, encoding the L protein which functions as the viral RNA-dependent RNA polymerase [12], and both M and S RNAs are ambisense. The M RNA encodes both glycoproteins (G_N and G_C) and the movement protein, NSm [13-16]. The S RNA encodes the nucleocapsid (N) protein and a RNA silencing suppressor, NSs [17-20]. The TSWV genome is encapsidated by N protein forming the ribonucleoproteins (RNPs) with a few copies of the L protein in each virus particle [7].

Although TSWV can be maintained in the laboratory through mechanical inoculation, it is transmitted in nature by insect vectors commonly known as thrips (Order Thysanoptera, Family *Thripidae*). Five species of *Frankliniella* and two species of *Thrips* are reported to be the vectors of TSWV [6]. Among these species, the western flower thrips, *Frankliniella occidentalis* Pergande, is the most efficient vector of TSWV and it has a worldwide distribution. TSWV is transmitted by thrips vectors in a persistent propagative manner, and the midgut cells and primary salivary glands are two major tissues in which TSWV replicates [21, 22]. Only thrips that acquire virus during the early larval stage are inoculative as adults [22-24]. Because the role of the viral components of the TSWV-*F. occidentalis* have been characterized, we sought to identify thrips proteins that interact directly with structural

components of the virion. Using gel overlay assays to identify first instar (L1) larval proteins that bind to purified virions or the G_N attachment protein, we discovered six TSWV interacting proteins (TIPs) from *F. occidentalis*. Identification of these proteins using mass spectrometry was followed with secondary assays to validate the interactions. Two TIPs specifically interacted with the viral glycoprotein G_N – the protein that plays a role in binding and entry into vector cells [25] – and co-localized with TSWV at the midgut of larval thrips, suggestive of molecules that may serve as receptors. These proteins represent the first thrips proteins that bind to TSWV proteins, and these novel discoveries provide insights toward a better understanding of the molecular interplay between vector and virus.

Results

Identification of bound *F. occidentalis* larval proteins using overlay assays

Proteins extracted from first instar larvae bodies were separated by 2-D electrophoresis and overlay assays were performed with purified TSWV virions or recombinant G_N glycoprotein to identify bound thrips proteins. Virions identified a total of eight proteins spots (Fig 1) - three occurred consistently in all four biological replicates, while five were present in three. Mass spectrometry and subsequent peptide sequence analysis against a 454-transcriptome database (*Fo* Seq) identified one to four different transcript matches per spot (Table 1), where in four cases, the same putative transcript matched peptides in more than one spot. Using recombinant G_N glycoprotein, 11 protein spots were detected in both biological replicates of the assay (Fig 2), and each spot was comprised of a single protein (single transcript match) occurring in multiple spots - there were a total of two different G_N-interacting proteins represented by the 11 spots (Table 2). In an additional gel overlay assay using virus-free plant extract (mock purification) obtained from healthy *D. stramonium*

plants, no protein spots above the antibody control were detected (data not shown).

Table 1. Identification of *Frankliniella occidentalis* larval proteins bound to purified virions of *Tomato spotted wilt virus* in two-dimensional (2-D) gel overlays.

Spot Number	*Fo* Seq contig match[a]	Mascot score ($P < 0.05$)	Percent coverage[b]	Number of matched peptides	Peptide sequence(s)	Blastx annotation[c] ($E < 10^{-20}$)	Conserved motifs ($E < 10^{-10}$)
1	contig01248	279	37%	4	R.AQQPYQQYLQNQQFQNYQQR.A R.AAAAPILQYSNDVNPDGSFQYSYQTGDGISAQAAGFTR.N K.DAEAQVVQGSYSYTGPDGVVYTVNYIADENGYR.A K.ALPYYNQQQATYQQQQAAYQR.P	endocuticle structural glycoprotein	Chitin_bind_4
	CL4854Contig1	363	29%	7	R.VFFDMTVDGQPAGR.I R.ALCTGEQGFGYK.G R.VIPNFMCQGGDFTNHNGTGGK.S R.KFADENFQLK.H K.HTGPGIMSMANAGPNTNGSQFFITTVK.T K.TSWLDNKHVVFGSVIEGMDVVK.K K.HVVFGSVIEGMDVVK.K	cyclophilin	Cyclophilin_ABH
2	contig01248	77	10%	1	K.DAEAQVVQGSYSYTGPDGVVYTVNYIADENGYR.A	endocuticle structural glycoprotein	Chitin_bind_4
3	contig00018	196	25%	4	R.FGGALGGYNLAQTSQYHIQTDEGPER.Y R.LEDGTVVGTYGWVDADGYLR.L R.PYYPSSTPAVSLVSSTPR.P R.PYYPTSTPAVVSSTPR.P	uncharacterized, similar to cuticular protein	Chitin_bind_4
	contig14634	134	22%	3	R.GYISELPGTYDANSNSVIPEYDGIAVTHNGFR.Y K.AGSFGYVDPFGIR.R R.VIYYNTSPGSGFQVR.K	uncharacterized, similar to cuticular protein	none identified
	CL4900Contig1	113	10%	3	R.GYISELPGTYDASSNSVIPEYDGIAVTHNGFR.Y K.AGSFGYVDPFGIR.R R.VIYYNTSPGSGFQVR.K	uncharacterized, similar to cuticular protein	Chitin_bind_4
4	CL1591Contig1	76	5%	1	K.QESVYTAAQPAISTYK.K	flexible cuticular protein	Chitin_bind_4
5	CL1591Contig1	89	5%	1	K.QESVYTAAQPAISTYK.K	flexible cuticular protein	Chitin_bind_4
6	CL4854Contig1	615	30%	9	R.VFFDMTVDGQPAGR.I R.ALCTGEQGFGYK.G R.VIPNFMCQGGDFTNHNGTGGK.S R.KFADENFQLK.H K.FADENFQLK.H K.FADENFQLKHTGPGIMSMANAGPNTNGSQFFITTVK.T K.HTGPGIMSMANAGPNTNGSQFFITTVK.T K.HVVFGSVIEGMDVVK.K K.KVVVADCGQLS	cyclophilin	Cyclophilin_ABH

7	CL4706Contig1	554	47%	17	R.GNPTVEVDLVTELGLFR.A R.AAVPSGASTGVHEALELR.D K.AIDNVNNIIAPELIK.S K.EIDELMLK.L K.LGANAILGVSLAVCK.A K.HIADLAGNTNIILPTPAFNVINGGSHAGNK.L K.LAMQEFMILPTGASSFK.E K.FGLDSTAVGDEGGFAPNILNNK.E K.EGLTLIIDAIAK.A K.VEIGMDVAASEFYK.D K.VEIGMDVAASEFYKDGQYDLDFK.N K.DGQYDLDFKNPNSDK.S K.LTDLYMEFIK.E K.EFPMVSIEDPFDQDHWDAWTTITGK.T K.TNIQIVGDDLTVTNPK.R K.VNQIGSVTESIQAHLLAK.K R.SGETEDTFIADLVVGLSTGQIK.T	enolase	Metal_binding
	contig12136	96	24%	2	R.QGDVVQGSYSLVEPDGSR.R R.TVEYTADPVNGFNAVVHK.D	cuticular protein	Chitin_bind_4
	contig14594	102	3%	1	R.TVDYTADPVNGFNAVVR.K	nuclear cap-binding protein	*RRM_NCPB2; Chitin_bind_4
	CL504Contig1	113	19%	2	K.AAVAVDTDYDPNPSYNYAYDIHDSLTGDAK.S R.TVEYTADPVNGFNAVVHK.E	cuticular protein	Chitin_bind_4
8	CL4706Contig1	407	43%	15	R.GNPTVEVDLVTELGLFR.A R.AAVPSGASTGVHEALELR.D K.AIDNVNNIIAPELIK.S K.HIADLAGNTNIILPTPAFNVINGGSHAGNK.L K.LAMQEFMILPTGASSFK.E K.FGLDSTAVGDEGGFAPNILNNK.E K.EGLTLIIDAIAK.A K.VEIGMDVAASEFYK.D K.VEIGMDVAASEFYKDGQYDLDFK.N K.DGQYDLDFKNPNSDK.S K.LTDLYMEFIK.E K.EFPMVSIEDPFDQDHWDAWTTITGK.T K.TNIQIVGDDLTVTNPK.R K.VNQIGSVTESIQAHLLAK.K R.SGETEDTFIADLVVGLSTGQIK.T	enolase	Metal_binding
	CL504Contig1	99	12%	1	K.AAVAVDTDYDPNPSYNYAYDIHDSLTGDAK.S	cuticular protein	Chitin_bind_4

[a]*de novo*-assembled contigs from *F. occidentalis* transcriptome derived by Roche 454/Sanger EST library hybrid (52)
[b]highest percent coverage obtained among the three picking gels used to collect protein spots for identification using ESI mass spectrometry
[c]NCBI Blastx search of the non-redundant protein database with the matching *Fo* nucleotide sequence contig query
*chimeric contig (= ambiguous annotation) - domains occur in opposite orientation on different ORFs

Table 2. Identification of *Frankliniella occidentalis* larval proteins bound to recombinant glycoprotein-N (G_N) in two-dimensional (2-D) gel overlays.

Spot Number	*Fo* Seq contig match[a]	Mascot score ($P < 0.05$)	Percent coverage[b]	Number of matched peptides	Peptide sequence(s)	Blastx annotation[c] ($E < 10^{-20}$)	Conserved motifs ($E < 10^{-10}$)
1	CL4310Contig1	595	27%	12	R.AAELSSILEER.I K.NIQADEMVEFSSGLK.G K.GMALNLEPDNVGIVVFGNDK.L K.GMALNLEPDNVGIVVFGNDKLIK.E R.TGAIVDVPVGDDLLGR.V K.TALAIDTIINQQR.F K.YTIIVAATASDAAPLQYLAPYSGCAMGEYFR.D K.HALIIYDDLSK.Q R.EAYPGDVFYLHSR.L R.EVAAFAQFGSDLDAATQQLLNR.G K.QGQYVPMAIEEQVAVIYCGVR.G K.IVTDFLASFNAASK	mitochondrial ATP synthase α subunit	AtpA
2	CL4310Contig1	302	12%	5	K.GMALNLEPDNVGIVVFGNDK.L R.TGAIVDVPVGDDLLGR.V R.VVDALGDAIDGK.G K.HALIIYDDLSK.Q K.IVTDFLASFNAASK	mitochondrial ATP synthase α subunit	AtpA
3	CL4382Contig1	633	43%	9	R.SSVVSQSVPVVSK.T K.SVPQYQQQYQTVSQYQSVPQYQQQVVVK.S K.SVPQYQQQVVVK.S K.SAPVYSQVHHVVEQQAAPVLLR.H R.TAFVPQYDSVSVSASAQPK.Y K.ILSQVQEFDPAGIYR.V R.VNFQTENGIQSAETGSVK.D R.ASGAHLPQVPEEIQR.S R.SLELNAAQPQKYDQDGNLVSQF	endocuticle structural glycoprotein	Chitin_bind_4
4	CL4382Contig1	137	15%	3	R.SSVVSQSVPVVSK.T K.SVPQYQQQYQTVSQYQSVPQYQQQVVVK.S R.VNFQTENGIQSAETGSVK.D	endocuticle structural glycoprotein	Chitin_bind_4
5	CL4382Contig1	169	22%	6	R.SSVVSQSVPVVSK.T K.SVPQYQQQVVVK.S R.VNFQTENGIQSAETGSVK.D R.ASGAHLPQVPEEIQR.S R.AAAEHGVAIVCPDTSPR.G K.ACQAVNMPVVLQMR.E	endocuticle structural glycoprotein	Chitin_bind_4
6	CL4382Contig1	1,154	53%	11	R.SSVVSQSVPVVSK.T K.SVPQYQQQYQTVSQYQSVPQYQQQVVVK.S K.SVPQYQQQVVVK.S K.SAPVYSQVHHVVEQQAAPVLLR.H R.HVEQEIPAYQSVQHVHQPVYQSVQHVAAHHVAAPVVSR.T R.TAFVPQYDSVSVSASAQPK.Y K.ILSQVQEFDPAGIYR.V R.VNFQTENGIQSAETGSVK.D	endocuticle structural glycoprotein	Chitin_bind_4

					R.VNFQTENGIQSAETGSVKDIQAK.D R.ASGAHLPQVPEEIQR.S R.SLELNAAQPQKYDQDGNLVSQF		
7	CL4382Contig1	413	74%	8	R.SSVVSQSVPVVSK.T K.SVPQYQQQYQTVSQYQSVPQYQQQVVVK.S K.SVPQYQQQVVVK.S R.TAFVPQYDSVSVSASAQPK.Y R.VNFQTENGIQSAETGSVK.D R.VNFQTENGIQSAETGSVKDIQAK.D R.ASGAHLPQVPEEIQR.S R.SLELNAAQPQKYDQDGNLVSQF	endocuticle structural glycoprotein	Chitin_bind_4
8	CL4382Contig1	355	29%	7	R.SSVVSQSVPVVSK.T K.SVPQYQQQYQTVSQYQSVPQYQQQVVVK.S K.SVPQYQQQVVVK.S R.VNFQTENGIQSAETGSVK.D R.VNFQTENGIQSAETGSVKDIQAK.D R.ASGAHLPQVPEEIQR.S R.SLELNAAQPQKYDQDGNLVSQF	endocuticle structural glycoprotein	Chitin_bind_4
9	CL4382Contig1	155	5%	2	R.VNFQTENGIQSAETGSVK.D R.VNFQTENGIQSAETGSVKDIQAK.D	endocuticle structural glycoprotein	Chitin_bind_4
10	CL4382Contig1	130	4%	1	R.VNFQTENGIQSAETGSVK.D	endocuticle structural glycoprotein	Chitin_bind_4
11	CL4382Contig1	150	13%	7	R.SSVVSQSVPVVSK.T K.SVPQYQQQYQTVSQYQSVPQYQQQVVVK.S K.SVPQYQQQVVVK.SR.VNFQTENGIQSAETGSVK.D R.TAFVPQYDSVSVSASAQPK.Y R.VNFQTENGIQSAETGSVK.D R.VNFQTENGIQSAETGSVKDIQAK.D R.ASGAHLPQVPEEIQR.S	endocuticle structural glycoprotein	Chitin_bind_4

[a]*de novo*-assembled contigs from *F. occidentalis* transcriptome derived by Roche 454/Sanger EST library hybrid (52)
[b]highest percent coverage obtained among the three picking gels used to collect protein spots for identification using ESI mass spectrometry
[c]NCBI Blastx search of the non-redundant protein database with the matching *Fo* nucleotide sequence contig query

Annotation of six candidate TSWV-interacting proteins

Our stringent sequence-filtering criteria retained four different virion-interacting proteins [endocuticle structural glycoprotein: endoCP-V (contig01248, GenBank accession: MH884756); cuticular protein: CP-V (CL4900Contig1, MH884758), cyclophilin (CL4854Contig1, MH884760), and enolase (CL4706Contig1, MH884759), Table 1] and two G_N-interacting proteins [mitochondrial ATP synthase α (CL4310Contig1, MH884761) and endocuticle structural glycoprotein; endoCP-G_N (CL4382Contig1, MH884757), Table 2] to move forward to validation and biological characterization. Collectively, these six protein candidates are referred to as 'TSWV-Interacting Proteins' or TIPs and their putative identifications and sequence features are shown in Table 3. Blastp analysis of the predicted, longest complete ORFs confirmed their annotations and putative sequence homology to proteins in other insects. The three cuticle-associated proteins (endoCP-G_N, endoCP-V, and CP-V) contained predicted signal peptide sequences, indication of secreted proteins, and a chitin-binding domain (CHB4). Pairwise alignments (Blastp) between the ORFs of these three cuticle proteins and the partial CPs and endoCPs identified in the gel overlays revealed diversity in these thrips proteins; three had no matches to others, and where matches occurred, % identities ranged from 53% – 67%, covering 30% – 49% of the queries, with e-values ranging from 2.4×10^{-2} – 3.6×10^{-24}. The only exception was the CP-V and contig00018 alignment, which appeared to be 100% identical along the entire length of contig00018 ($E = 2.6 \times 10^{-162}$). The other three TIPs (cyclophilin, enolase and mATPase) contained motifs characteristic of these proteins (Table 3).

Table 3. Final candidate list of six TSWV-interacting proteins (TIPs)[a] from larval *Frankliniella occidentalis* to move forward to validation and biological characterization.

Putative protein	*Fo* Seq contig match[b]	ORF length[c] (nt/aa)	Signal peptide[d] (aa position)	Conserved domains[e]			Top Genbank match[f] (% coverage, % identity, E)
				Name	Position (aa)	E-value	
Cuticular protein-V (CP-V)	CL4900Contig1	1,302/434	1-18	Chitin_bind_4	447-92	$5.7x10^{-6}$	XP_017786818.1: PREDICTED: cell surface glycoprotein 1 [*Nicrophorus vespilloides*] (94%, 44%, $1x10^{-85}$)
Endocuticle structural glycoprotein-G_N (endoCP-G_N)	CL4382Contig1	852/283	1-15	Chitin_bind_4	190-246	$7.5x10^{-11}$	XP_018334183.1: endocuticle structural glycoprotein SgAbd-2-like [*Agrilus planipennis*] (33%, 53%, $4x10^{-22}$)
Endocuticle structural glycoprotein-V (endoCP-V)	contig01248	522/173	1-17	Chitin_bind_4	63-119	$1.4x10^{-18}$	XP_022906571.1: endocuticle structural glycoprotein SgAbd-2-like [Onthophagus taurus] (63%, 58%, $2x10^{-35}$)
Cyclophilin (peptidyl-prolyl cis-trans isomerase)	CL4854Contig1	618/205	None	cyclophilin_ABH_like PpiB Pro_isomerase	44-202 57-196 47-201	$2.3x10^{-120}$ $2.6x10^{-63}$ $1.2x10^{-62}$	XP_019753975.1: PREDICTED: peptidyl-prolyl cis-trans isomerase [*Dendroctonus ponderosae*] (99%, 75%, $2x10^{-109}$)
Enolase	CL4706Contig1	1,302/433	None	PLN00191 enolase Eno Enolase_C	3-433 5-417 6-431 143-433	0 0 0 0	XP_019767728.1: PREDICTED: enolase-like [*Dendroctonus ponderosae*] (99%, 87%, 0)
Mitochondrial ATP synthase α	CL4310Contig1	1,665/554	None	PRK09281 AtpA F1_ATPase_alpha ATP-synt_ab	45-551 45-553 135-416 190-413	0 0 0 $6.1x10^{-117}$	XP_023718907.1: ATP synthase subunit alpha, mitochondrial [*Cryptotermes secundus*] (99%, 89%, 0)

[a]sequences deposited into National Center for Biotechnology Information (NCBI) GenBank with the following accessions: CP-V (MH884758), endoCP-G_N (MH884757), endoCP-V (MH884756), cyclophilin (MH884760), enolase (MH884759), and mitochondrial ATP synthase α (MH884761).

[b]*de novo*-assembled contigs from *F. occidentalis* transcriptome derived by Roche 454/Sanger EST library hybrid (52)

[c]prediction by NCBI ORF Finder (https://www.ncbi.nlm.nih.gov/orffinder/)

[d]prediction by Signal P (http://www.cbs.dtu.dk/services/SignalP/)

[e]prediction by NCBI Batch Web CD Search Tool (https://www.ncbi.nlm.nih.gov/Structure/bwrpsb/bwrpsb.cgi) (CDSEARCH/cdd v3.16); E-value cut-off = 10^{-5}, only specific hits shown

[f]Blastp search of NCBI nr protein database against TIP ORF as of August 06, 2018; top match indicates highest alignment (max) score

196 **Classification of cuticular TIPs**

197 All three cuticular TIPs were classified as members of the Cuticle Protein - R&R
198 Consensus motif (CPR) family [26] based on the occurrence of one RR extended consensus
199 CHB4, with both endoCP-G_N (E = 4 x 10^{-18}) and endoCP-V (E = 1 x 10^{-26}) predicted to
200 belong to the RR1 group, and CP-V weakly supported (E = 5x10^{-6}) to belong to the RR2
201 group of CPRs. All three sequences were phylogenetically placed into the RR1 major clade
202 with strong bootstrap support (82%, S1 Fig) in relation to other *F. occidentalis* CPRs
203 previously found to be downregulated in TSWV-infected first instar larvae [27] and CPRs of
204 other insect species. Within the RR1 clade, the CP-V CHB4 domain clustered with a CP of
205 the small brown planthopper, *Laodelphax striatella* (KC485263.1, CprBJ), reported to bind to
206 the nucleocapsid protein pc3 of rice stripe virus (RSV) during infection of the vector [28] and
207 which was predicted (E = 5 x 10^{-7}) to be classified in the RR1 group.
208

209 **Validation of gel overlay protein-protein interactions using yeast two-hybrid analysis**

210 Both Gal4 transcriptional activator-based and membrane-based yeast two-hybrid
211 (MbY2H) systems were applied and repeated three times to validate the gel-overlay
212 interactions between the six candidate TIPs and TSWV nucleocapsid (N) protein and
213 glycoprotein G_N. Given TSWV N is soluble, both Y2H systems were applied, and both
214 systems revealed strong interactions between TSWV N and each of the six TIPs; only the
215 MbY2H assay results are presented in Fig 3A. The N-TIPs interactions were confirmed by β-
216 galactosidase assay (S1 Table).

217 We used the MbY2H system to validate TSWV G_N interactions with the TIPs due to the
218 presence of a transmembrane domain near the C-terminus of TSWV G_N. The interaction
219 between G_N and endoCP-G_N was consistent and strong based on the number of colonies

growing on QDO - more than 1,000 colonies on all QDO plates for all replicates (Fig 3B) - and this interaction was confirmed by β-galactosidase assay (S2 Table). We detected a weak interaction (average of 15 colonies) between G_N and cyclophilin, however, seven of nine colonies tested by β-galactosidase assay were positive. Consistent with the gel overlay findings, the remaining four TIPs showed no interaction with G_N using MbY2H.

The non-conserved region of endoCP-G_N binds TSWV G_N

Given the role of G_N as the viral attachment protein in the larval thrips midgut epithelium [7, 10] and the confirmed direct interaction between endoCP-G_N and TSWV G_N, there was interest in broadly identifying the amino acid region in the endoCP-G_N sequence that binds viral G_N. We hypothesized that the non-conserved region of endoCP-G_N (N-terminal region up to 176 aa or 189 aa) and not the CHB4 motif might play an important role in the interaction with TSWV G_N. Using the MbY2H system, it was determined that the non-conserved region of the endoCP-G_N sequence had as strong of an interaction with TSWV G_N as the complete endoCP-G_N sequence (Fig 3C and S2 Table) - more than 500 colonies on each QDO plate for each experimental replicate – while the predicted CHB4 motif alone (amino acid positions 190-284) or CHB4 plus few amino acids upstream (position 177-284)) did not show an interaction. The non-conserved endoCP-G_N sequence region was determined to have no significant matches to sequences in NCBI non-redundant nucleotide and protein databases.

Validation of interactions between TIPs and TSWV using BiFC

Before launching a BiFC analysis of candidate protein interactions *in planta*, it is critical to determine if position of a fused fluorescent protein tag (N- or C-terminus of the candidate

245 protein) affects the expression and/or localization of the fusion protein in cells. Furthermore,
246 it was expected that the signal peptides located on the N-terminus of the soluble (G_C-S and
247 G_N-S) and insoluble (G_C and G_N) TSWV glycoproteins, and the cuticular TIPs (CP-V,
248 endoCP-V, endoCP-G_N), would preclude placement of tags at the N-terminus of these
249 proteins. We determined that position of the GFP tag on TSWV N did not appear to effect
250 expression or localization of the fusion protein in *N. benthamiana* cells. However, GFP fused
251 to the N-terminus of the glycoproteins (G_N, G_N-S, G_C and G_C-S), the cuticle TIPs (endoCP-
252 G_N and endoCP-V), and mATPase α produced weak signal or reduced mobility in the cell
253 (data not shown). Thus, protein localization and BiFC validation experiments were performed
254 with C-terminally fused TIPs.

255 The GFP-TIP fusion proteins displayed some differences in their cellular localization
256 patterns (S2 Fig). Cyclophilin and mATPase α appeared to be localized to the nuclei and
257 along the cell periphery, while enolase and CP-V were present in the membranes surrounding
258 the nuclei as well as the cell periphery. Both endoCP-G_N and endoCP-V had a punctate
259 appearance outside of the nucleus. All three cuticular TIPs (CP-V, endoCP-G_N, endoCP-V)
260 formed small bodies that appeared to be moving along the endo-membranes of the cell,
261 consistent with secretion. All TIPs were co-localized with the ER marker; however, none
262 appeared to be co-localized with the Golgi marker (data not shown).

263 With a few exceptions, BiFC analysis validated the TSWV - TIP interactions (Fig 4).
264 Consistent with the MbY2H findings, TSWV N protein interacted with cyclophilin,
265 mATPase α, CP-V, endoCP-V and endoCP-G_N, and G_N interacted with endoCP-G_N. Contrary
266 to MbY2H results, there was no apparent interaction between TSWN N and enolase, and G_N
267 was determined to have additional interactions with enolase and endoCP-V. The steric
268 constraints imposed by the position (C- or N-terminus) of the reporter in the BiFC (YFP half)
269 and MbY2H (Ubiquitin half) systems in plants vs yeast cells, respectively, may explain the

contrasting interactions. The soluble forms of the viral glycoproteins produced some varying results from their insoluble counterparts: G_N-S interacted with mATPase α and endoCP-V (and not endoCP-G_N), and G_C did not interact with any of the six TIPs but G_C-S interacted with Cp-V. All of the BiFC interactions were detected in the membranes surrounding the nuclei and at the cell periphery, generally consistent with the localization patterns of the GFP-fused TIPs as described for the localization experiment above (S2 Fig).

In vivo localization of TIPs in *F. occidentalis* tissues

Specific antisera raised against each confirmed TIP was used in immunolabeling experiments to localize protein expression in L1 tissues *in vivo*. Visualization by confocal microscopy revealed that all six TIPs were primarily localized at the foregut (esophagus), midgut (epithelial cells and visceral muscle), salivary glands (including both primary and tubular salivary glands), and Malpighian tubules (Fig 5), and this was the case in 100% of the dissected tissues treated with TIP-specific antisera. It was difficult to completely dissect and separate hindgut from the carcass without damaging the tissue, therefore, the localization of TIPs at the hindgut was unclear. All controls labeled with pre-immune serum for each TIP showed slightly higher background than the no antibody control, therefore, the confocal laser settings (power and percent/gain) were adjusted to remove any background fluorescence observed for these treatments. The bright field and merged images of these controls, depicting actin- and nuclei-labeling, are shown in S3 Fig.

In vivo co-localization of G_N-interacting TIPs and TSWV in *F. occidentalis* tissues

Virus acquisition experiments were conducted to determine localization of TSWV in relation to endoCP-G_N and cyclophilin expression in larval thrips. After each AAP (24, 48 and 72 hours of exposure), dissected tissues were incubated with TSWV and TIP-specific antisera and viewed by confocal microscopy. At the 24 hour-virus exposure, virus infection

was limited to a few midgut epithelial cells in the anterior region of the midgut (MG1) adjacent to the cardiac valve. With increasing virus exposure time, TSWV was observed in increasingly more of the epithelium and into the visceral muscle cells of MG1 (48 hrs and 72 hrs). Consistent with the localization of TIPs expressed in healthy young L1s obtained from the lab colony (Fig 5), cyclophilin and endoCP-G_N were expressed widely throughout larval midgut tissues (epithelial cells and visceral muscle) regardless of treatment (non-exposed and TSWV-infected) and exposure time to virus (Fig 6). Both TIPs were co-localized with virus (Fig 6), which was consistently observed for all of the TSWV G_N-labeled tissues examined (13, 9 and 15 intact tissues for endoCP-G_N experiments, and 7, 7, and 8 intact tissues for cyclophilin experiments for the three AAPs, respectively). Although TIPs were expressed throughout the entire midgut tissue system, not all epithelial cells were labeled positive for TSWV G_N, consistent with the normal progression of TSWV infection in thrips [29]. As for SGs, both TIPs were expressed in these tissues in both treatments, however no virus was detected in the SGs of the early second instar larvae comprising the 72-hr samples. At the confocal level, we did not detect a change in endoCP-G_N or cyclophilin expression in infected insects compared to non-infected insects. The no-virus controls - actin and nuclei-stained, bright field and the merged panels - are shown in S4 Fig.

Discussion

With the creation of transcriptome sequence resources for *F. occidentalis* and improved proteomics technologies, we have identified the first thrips proteins that bind directly to major structural proteins of TSWV. With particular relevance to viral attachment to epithelia, one TIP (endocuticle structural glycoprotein, endoCP-G_N) was confirmed consistently to interact directly with G_N, it was abundant in midgut and salivary gland tissues, and it co-localized with TSWV 24-hours post exposure at the anterior region of larval midguts - the

initial site of infection [29]. These data may be the first indication of a protein that serves 'receptor-like' roles in transmission biology of a plant-infecting member of the Bunyavirales. We narrowed down the G_N-binding region to the amino terminal region of endoCP-G_N excluding the conserved CHB4 domain, setting the stage for future work to decipher the essential amino acids within the non-conserved region necessary to establish the interaction. With regards to other virus activities mediated by bunyavirus nucleocapsid (N) proteins in host cells, the confirmed affinity of TSWV N to five of the six TIPs, including endoCP-G_N, may indicate interactive host factors involved with N-associated roles, such as viral transcription, replication, and/or virion maturation in animal [30, 31] and plant hosts [32, 33]. Evidence of the cell peripheral (mATPase, cyclophilin, endoCP-G_N, endoCP-V, CP-V) or perinuclear (cyclophilin) accumulation and co-localization of these five TIPs with N in the BiFC assay support this hypothesis.

The most enriched thrips proteins in the initial screen for those bound to virions or G_N (Table 1 and 2, 72%) were cuticular proteins. Cuticular proteins are well characterized as major components of insect hard and soft cuticles [34, 35]. Soft cuticles have been documented to line the insect foregut and hindgut [36, 37], and an EM study documented cuticle lining of the accessory and primary salivary gland (SG) ducts of *F. occidentalis* [38]. In silico sequence analysis of the three cuticular TIPs (CP-V, endo-V, endo-G_N) revealed conserved CHB4 domains (R&R) suggesting their binding affinity to chitin (heteropolymer of N-acetyl-β-D-glucosamine and glucosamine), also a major component of cuticles and peritrophic membranes (PM) lining the midgut epithelium of most insects [39]. Hemipteran and thysanopteran midguts lack PMs, and are instead lined with perimicrovillar membranes (PMM) [40, 41] - these structures have been reported to contain lipoproteins, glycoproteins and carbohydrates [42, 43] and more recently, one study documented the occurrence and importance of chitin in the PMM of *Rhodnius prolixus* (kissing bug) midguts, marking the

first hemipteran midgut reported to contain chitin [44]. Since all three cuticular TIPs were highly expressed in the midgut and SGs of larval *F. occidentalis* in the present study, we hypothesize that chitin or chitin-like structures may impregnate the thrips PMM and SG-linings, forming a matrix with endoCPs - however, this remains to be empirically determined. Alternatively, the thrips TIPs annotated as cuticle proteins with predicted chitin-binding domains may have yet-undescribed functions in insect biology.

Cuticular proteins are emerging as important virus interactors and responders in diverse vector-borne plant virus systems. A CP of the hemipteran vector, *Laodelphax striatellus*, was found to interact with the nucleocapsid protein (pc3) of *Rice stripe virus* (genus *Tenuivirus,* order *Bunyavirales*) and was hypothesized to be involved in viral transmission and to possibly protect the virus from degradation by a host immune response in the hemolymph [28]. Recently, a CP of another hemipteran vector, *Rhopalosiphum padi*, was identified to interact with *Barley yellow dwarf virus*-GPV (genus *Luteovirus*, family *Luteoviridae*) readthrough protein, and the gene transcript of this particular CP was differentially expressed in viruliferous compared to virus-free aphids [45]. At the transcript level, thrips cuticular proteins of different types - including the thrips CPRs used in the present study to phylogenetically place the three cuticular TIPs - were identified to be downregulated in TSWV-infected first instar larvae [27]. Although the three cuticular TIPs identified in the present study were not reported in the previous study to be differentially-responsive to virus, both implicate cuticle-associated proteins during the early infection events of TSWV in the thrips vector.

Cyclophilins, also known as peptidyl-prolyl cis-trans isomerases, are ubiquitous proteins involved in multiple biological processes, including protein folding and trafficking, cell signaling, and immune responses [46]. They have also been shown to promote or prevent virus infection [47, 48], for example, cyclophilin A was found to bind to viral RNA to inhibit

368 replication of *Tomato bushy stunt virus* (*Tombusviridae*: *Tombusvirus*) in plant leaf cells [49],
369 while cyclophilins of the aphid vector *Schizaphis graminum* have been shown to play an
370 important role in *Cereal yellow dwarf virus* (*Luteoviridae*: *Polerovirus*) transmission [50].
371 Interactions between the thrips cyclophilin TIP (with N and G_N) documented in the present
372 study may affect similar virus processes, such as virus replication and maturation, or thrips
373 transmission and vector competence [50, 51]. The same cyclophilin was determined to be
374 down-regulated in *F. occidentalis* first instar larvae during TSWV infection [52], adding to
375 the body of evidence that viruses modulate expression of cyclophilins [53-58]. Others have
376 proposed that negative strand virus matrix proteins – structural proteins that package viral
377 RNA - evolved from cyclophilins [59]; however, bunyaviruses do not encode a matrix
378 protein. One hypothesis for the direct interaction between the cyclophilin TIP with N and G_N
379 may be to facilitate RNP packing into the virus particle, perhaps serving as a surrogate matrix
380 protein for TSWV.

381 Like cyclophilins, enolases of diverse hosts have been identified as both responsive to
382 and interactive partners with viruses. In general, enolases are essential metalloenzymes that
383 catalyze the conversion of 2-phosphoglycerate (2-PGE) to phosphoenolpyruvate (PEP) in the
384 glycolytic pathway for energy metabolism [60]. Some are matrix metalloproteases known to
385 cleave cell surface receptors, modulate cytokine or chemokine activities, or release apoptotic
386 ligands by degrading all types of extracellular matrix proteins, such as collagen, elastin,
387 fibronectin, laminin, gelatin, and fibrin [61]. The enolase TIP identified in the present study
388 was previously reported to be up-regulated in L1 bodies infected with TSWV [52], as was the
389 case for enolase in response to RSV in bodies of the hopper vector, *L. striatellus* [62]. In the
390 case of flaviviruses, *Aedes aegypti* enolase was shown to directly interact with purified virus
391 and recombinant envelope GP of dengue virus [63] and West Nile virus envelope protein
392 [64]. The localization of this enolase in brush border membrane vesicles of this mosquito

393 species [65] strengthens the case for a proposed receptor role in virus entry into vector
394 mosquito midguts. Other insect-virus studies have proposed a role for enolase in antiviral
395 defense [61] and tracheal basal laminal remodeling aiding in virus escape from the gut [66].
396 If remodeling of the midgut basal lamina via enolase interactions occurs in TSWV-infected
397 larval thrips, that could be one hypothesis supporting dissemination of TSWV from the larval
398 midgut into the principal SGs [24].

399 The other TIP known to play a role in energy production is mitochondrial ATP synthase
400 α subunit. The multi-subunit enzyme mATPase is responsible for generating the majority of
401 cellular ATP required by eukaryotes to meet their energy needs. As with the other non-
402 cuticle TIPs, mATPase α subunit was previously identified to be differentially-abundant (up-
403 regulated) under TSWV infection [52], as was the case for RSV-infected *L. striatellus* vector
404 hoppers [62]. Mitochondria have been also been implicated in virus-host biology. For
405 example, *African swine fever virus* (ASFV; *Asfarviridae*: *Asfivirus*) has been shown to induce
406 migration of mitochondria to the periphery of viral factories [67], possibly suggesting that
407 mitochondria supply energy for viral morphogenetic processes. The finding that two TIPs in
408 the present study have ontologies in energy production and metabolism suggests that
409 perturbation or direct interactions with these host proteins may be required for the successful
410 infection of *F. occidentalis* by TSWV.

411 The discovery of six TIPs is a significant step forward for understanding thrips
412 interactions with TSWV. The first evidence of TSWV protein-thrips protein interactions was
413 presented 20 years ago [68] and the proteins described herein are the first thrips protein
414 documented to interact directly with the major structural proteins (N, G_N, G_C). In other
415 eukaryotes, the six interacting proteins have biological functions that point to their roles in
416 facilitating the virus infection/replication cycle by acting as a receptor or other essential step
417 in the virus lifecycle, and/or host-response via a defense mechanism. The virus-host systems

418 that have defined functions for analogous TIPs include plant viruses, arboviruses, and
419 animal/human viruses, and the findings described here provide a framework for further
420 exploration and testing of new hypotheses regarding their roles in TSWV-thrips interactions.

421 ## Materials and methods

422 ### Insect rearing and plant and virus maintenance

423 The *F. occidentalis* colony was established from insects collected on the island of Oahu,
424 HI, and was maintained on green beans (*Phaseolus vulgaris*) at 22ºC (±2ºC) under laboratory
425 conditions as previously described [69]. Thrips were synchronized based on their
426 developmental stages. For the localization and bimolecular fluorescence complementation
427 (BiFC) experiments, wildtype and transgenic *Nicotiana benthamiana* expressing CFP:H2B or
428 RFP:ER [70] were grown in a growth chamber at 25ºC with a 14-hour light at 300µM
429 intensity and 10-hour dark cycle. TSWV (isolate TSWV-MT2) was maintained by both
430 mechanical inoculation and thrips transmission using *Datura stramonium* and *Emilia*
431 *sonchifolia*, respectively [21]. To avoid generation of a virus isolate with an insect
432 transmission deficiency, the virus was mechanically passaged only once. The single-pass
433 mechanically-inoculated symptomatic *D. stramonium* leaves were used for insect acquisition
434 of TSWV. Briefly, synchronized *F. occidentalis* first instar larvae (0-17-hour old) were
435 collected and allowed an acquisition access period (AAP) on *D. stramonium* for 24 hours.
436 After acquisition, *D. stramonium* leaves were removed and these larvae were maintained on
437 green beans until they developed to adults. Viruliferous adults were transferred onto clean *E.*
438 *sonchifolia* for two days. After inoculation, thrips and inoculated *E. sonchifolia* plants were
439 treated with commercial pest strips for two hours before the plants were moved to the
440 greenhouse for TSWV symptom development. The thrips-transmitted, TSWV symptomatic
441 *E. sonchifolia* leaves were only used for mechanical inoculation.

442 **TSWV purification**

443 Mechanically inoculated *D. stramonium* leaves were used for TSWV purification via
444 differential centrifugation and a sucrose gradient. Symptomatic leaves were homogenized
445 in extraction buffer (0.033 M KH_2PO_4, 0.067 M K_2HPO_4, and 0.01 M Na_2SO_3) in a 1:3
446 ratio of leaf tissue to buffer. The homogenate was then filtered through four layers of
447 cheesecloth, and the flow through was centrifuged at 7,000 rpm for 15 min using the
448 Sorvall SLA 1500 rotor. To remove the cell debris, the pellet was resuspended in 65 mL
449 0.01 M Na_2SO_3 and was centrifuged again at 8,500 rpm for 20 min using the Sorvall SS34
450 rotor. The supernatant that contained the virions was centrifuged for 33 min at 29,300 rpm
451 using the 70 Ti rotor, and the pellet was resuspended in 15 mL 0.01 M Na_2SO_3 followed by
452 another centrifugation at 9,000 rpm for 15 min using the Sorvall SS34 rotor. The
453 centrifugation series was repeated one additional time. The pellet was resuspended and
454 loaded on a sucrose gradient (10 to 40% sucrose), which was centrifuged for 35 min at
455 21,000 rpm using the SW28 rotor. The virion band was collected and centrifuged for 1
456 hour at 29,300 rpm using the 70 Ti rotor. The pellet was resuspended in 100 to 200 µl of
457 0.01 M Na_2SO_3. All centrifugation steps were performed at 4ºC to prevent virion
458 degradation. The purified virus was quantified using the bicinchoninic acid (BCA) protein
459 assay kit (ThermoFisher Scientific, Waltham, MA, USA) following the manufacturer's
460 instructions.

461 ***F. occidentalis* L1 total protein extraction, quantification and two-dimensional (2-D)**
462 **electrophoresis**

463 Total proteins from age-synchronized healthy larval thrips (0-17-hour old) were
464 extracted using the trichloroacetic acid-acetone (TCA-A) method [71, 72]. Briefly, whole
465 insects were ground using liquid nitrogen, and were dissolved in 500 µl TCA-A extraction
466 buffer (10% of TCA in acetone containing 2% β-mercaptoethanol). This mixture was

incubated at -20ºC overnight and centrifuged at 5,000 *g*, 4ºC for 30 min. After 3 washes with ice-cold acetone then air-drying, the pellet was resuspended in 200 µl General-Purpose Rehydration/Sample buffer (Bio-Rad Laboratories, Hercules, CA, USA). The suspension was centrifuged at 12,000 *g* for 5 min and the protein supernatant was quantified using the BCA protein assay kit (ThermoFisher Scientific) following manufacturer's instructions. For each gel, 150 µg of total protein extract was applied to an 11-cm IPG strip (pH 3–10) for isoelectric focusing (IEF). The IEF, IPG strip equilibration and second dimension separation of proteins were performed under the same conditions described by Badillo-Vargas et al [52].

Overlay assays

To identify thrips proteins that bind to TSWV virions and recombinant glycoprotein G_N, we conducted gel overlay assays. For the purified virion overlays, the experiment was performed four times (biological replications); and for the G_N overlay, the experiment was performed twice. For probing the protein-protein interactions, each unstained 2-D gel was electro-transferred onto Hybond-C Extra nitrocellulose membrane (Amersham Biosciences, Little Chalfont, UK) overnight at 30 V (4ºC) in protein transfer buffer (48 mM Tris, 39 mM glycine, 20% methanol, and 0.037% SDS). Then, the membrane was incubated with blocking buffer (PBS, 0.05% Tween 20 and 5% dry milk) for 1h at room temperature on a rocker with a gentle rotating motion. Three different antigens were used to probe the thrips protein membranes: purified TSWV virions, recombinant glycoprotein G_N (*E. coli* expressed), and virus-free plant extract from a mock virus purification (negative control). An additional negative control blot (no overlay) treated with antibodies alone was included in each overlay replicate. For the virus and G_N treatments, 25 µg/mL and 3.5 µg/mL of purified TSWV virions and recombinant G_N glycoprotein, respectively, were incubated with membranes in blocking buffer at 4ºC overnight with gentle rotating motion. Membranes were washed three times using PBST and were incubated with polyclonal rabbit anti-TSWV G_N antiserum at

1:2,000 dilution in blocking buffer for 2 hours at room temperature [9, 29]. After washing with PBST, membranes were incubated with HRP-conjugated goat-anti rabbit antiserum at 1:5,000 dilution in blocking buffer for 1 hour at room temperature. The ECL detection system (Amersham Biosciences) was used for protein visualization following the manufacturer's instructions. The protein spots that were consistently observed on the membranes were first compared with those proteins spots that interacted with antibody-only blots (Fig 1A and Fig 2A) and virus-free plant extract blots, and then they were pinpointed on the corresponding Coomassie Brilliant Blue G-250-stained 2-D gels for spot picking.

Identification of TIPs

Protein spots that were consistently identified in the 2-D gel overlays were selected and manually picked for analysis. The picked proteins were processed and subjected to ESI mass spectrometry as previously described [31]. Protein spots (peptides) that had Mascot scores (Mascot v2.2) with significant matches ($P \leq 0.05$) to translated *de novo*-assembled contigs (all six frames) derived from mixed stages of *F. occidentalis* ("*Fo* Seq" 454-Sanger hybrid) [52] were identified and NCBI Blastx was performed on the contigs to provisionally annotate ($E < 10^{-10}$) the protein and to predict conserved motifs using the contig as the query and the NCBI non-redundant protein database as the subject.

A second round of TIP candidate selection was conducted for stringency in moving forward to cloning and confirmation of interactions. A contig sequence was retained if it contained a complete predicted ORF (*i. e.*, presence of both start and stop codons predicted with Expasy, Translate Tool, http://web.expasy.org/translate/) and had at least 10% coverage by a matching peptide(s) identified for a spot as predicted by Mascot. *i. e.* removal of proteins identified by a single peptide with less than 10% coverage to a *Fo* Seq contig and/or contigs with incomplete ORFs (lacking predicted stop codon). The translated ORFs were queried against the NCBI non-redundant protein database (Blastp), and CCTOP software

517 (http://cctop.enzim.ttk.mta.hu) [73] and SignalP 4.1 Server
518 (http://www.cbs.dtu.dk/services/SignalP/) [74] were used to predict the presence of
519 transmembrane domains and signal peptides, respectively. Prosite (http://prosite.expasy.org/)
520 was used to analyze putative post-translational modifications that may have affected
521 electrophoretic mobility of identical proteins in the overlay assays, i. e., same peptide
522 sequence or *Fo* Seq contig match identified for more than one protein spot.
523
524 **Classification and phylogenetic analysis of the three confirmed cuticular TIPs**
525 Given the apparent enrichment of putative cuticular proteins (CP) identified in the
526 overlay assays and the subsequent confirmation of three of those TIPs (CP-V, endoCP-G_N,
527 endoCP-V), it was of interest to perform a second layer of protein annotations. The ORFs
528 (amino acid sequence) of the three confirmed CP TIPs, 19 exemplar insect orthologous
529 sequences obtained from NCBI GenBank, and a significant collection of structural CP
530 transcripts previously reported to be differentially-expressed in TSWV-infected larval thrips
531 of *F. occidentalis* [27] were subjected to two complementary arthropod CP prediction tools.
532 CutProtFam-Pred (http://aias.biol.uoa.gr/CutProtFam-Pred/home.php) [75] was used to
533 classify each amino acid sequence by CP family – there are 12 described families for
534 arthropods, each distinguished by conserved sequence motifs shared by members [35] – and
535 CuticleDB (http://bioinformatics.biol.uoa.gr/cuticleDB) [76] was used to distinguish what
536 was found to be two enriched, chitin-binding CP families in our dataset: CPR-RR1 and CPR-
537 RR2, *i. e.*, R&R Consensus motif [26]. The sequences flanking the RR1 and RR2 predicted
538 chitin-binding domains were so divergent between the thrips CPs and across the entire set of
539 CPs (thrips and other insects) that alignments using full-length ORFs were ambiguous and
540 uninformative, thus illustrating the utility of the R&R Consensus for inferring evolutionary
541 history of CP proteins. The flanking sequences were trimmed manually, and the R&R

consensus sequences (RR1 and RR2) were aligned with MEGA7 [77] using ClustalW. Phylogenetic analyses were performed in MEGA7 using the Neighbor-Joining (NJ) method and the best substitution models determined for the data - Dayhoff matrix-based [78] or Jones Taylor Thorton (JTT) [79] methods for amino acid substitutions with Gamma distribution - to model the variation among sites. Bootstrap consensus trees (500 replicates) were generated by the NJ algorithm with pairwise deletion for handling gaps. The analysis involved 46 sequences and there were 95 amino-acid positions in the final dataset.

Cloning of candidate TIPs and TSWV genes

For generation of full-length clones of TIPs that were used in various protein-protein assays, total RNA was extracted from L1 thrips (0-17-hour old) using 1 ml Trizol Reagent (ThermoFisher Scientific), then 200 µl chloroform and was precipitated with 500 µl isopropanol. The RNA pellet was dissolved in nuclease-free water, and 1µg total RNA was used for cDNA synthesis using Verso cDNA Synthesis kit (ThermoFisher Scientific). The PCR was performed to amplify six identified TIP ORFs using high fidelity polymerase, FailSafe (Epicentre, Madison, WI, USA). The designed primers used are listed in S3 Table. Amplicons were cloned into pENTR-D/TOPO (ThermoFisher Scientific).

TSWV genes were also cloned to pENTR-D/TOPO, then recombined to different vectors using Gateway cloning techniques. Coding sequence of TSWV N gene was amplified from pBS-NC4.5 [80], while coding sequences of different glycoproteins, G_N, G_N-S, G_C, G_C-S were amplified from pGF7 [81]. Primers used for PCR were listed in S3 Table.

Gal4-based yeast two-hybrid (Y2H) assay

The Matchmaker Gold Yeast Two-Hybrid System (Takara Bio, Kusatsu, Shiga Prefecture, Japan) was used for validating interactions between TIPs and TSWV N. TSWV N and TIP ORFs were cloned from pENTR entry clones to pDEST-GBKT7 (The Arabidopsis

Information Resource, TAIR, Accession: 1010229696) and pDEST-GADT7 (TAIR, Accession: 1010229695), respectively, using Gateway LR Clonase II Enzyme Mix (Thermo Fisher Scientific). After Sanger sequencing confirmation, every subject plasmid pair, including one pDEST-GADT7-TIP and pDEST-GBKT7-N were co-transformed into yeast strain Y2HGold following the manufacturer's instructions. Briefly, yeast (Y2HGold) competent cells were freshly prepared following the manufacturer's instructions, then each purified plasmid pair (100ng / plasmid) were added into 100 µl yeast competent cells with 50 µg denatured Yeastmaker Carrier DNA and 50 µl PEG/LiAc. The mixture was incubated at 30ºC for 30 min with mixing every 10 min. Twenty microliters of dimethyl sulfoxide (DMSO) was then added into each reaction, and the cells were incubated at 42ºC for 20 min with mixing every 5 min. After centrifugation at 14,000 rpm for 15 sec, the supernatant was removed, and the pellet was resuspended in 1 ml YPDA media. The re-suspended cells were incubated at 30ºC for 90 min with shaking at 200 rpm. Cells were centrifuged at 14,000 rpm for 15 sec, and resuspended in 500 µl sterile 0.9% (w/v) NaCl, which was then spread and cultured on both SD–Leu/–Trp double dropout (DDO) and SD–Ade/–His/–Leu/–Trp quadruple dropout (QDO) media. The positive and negative control plasmid pairs used were pGADT7-T and pGBKT7-53, and pGADT7-T and pGBKT7-Lam, respectively. The entire experiment was performed three times.

Split-ubiquitin membrane-based yeast two-hybrid (MbY2H)

The MbY2H system was used to validate both TSWV G_N-TIPs and TSWV N-TIPs interactions identified in the gel overlays. The MbY2H system enables validation of interactions for soluble and integral membrane proteins. TSWV G_N and N coding sequences were cloned into the MbYTH vector pBT3-SUC, and six TIP ORFs were cloned to vector pPR3N using SfiI (Dualsystems Biotech, Schlieren, Switzerland). To identify the region of endoCP-G_N that binds to TSWV G_N using MbY2H, the amino acid sequence of endoCP-G_N

(284aa) was used to search against the NCBI non-redundant protein database using Blastp. The conserved CHB4 domain was located at C-termini of endoCP-G_N (amino acid 190-246). Therefore, the possible interacting domains, the non-conserved region of endoCP-G_N (1-189aa) and the conserved CHB4 domain (190-274aa), were individually cloned into pPR3N using the SfiI restriction site. Based on the Blastp results, the homologous sequences from other insect species encompassed some additional amino acids upstream of the CHB4 domain; therefore, we made an alternative construct that included the conserved CBH4 domain starting from amino acid 177. Hence, the coding sequence of 1-176aa and 177-284aa of endoCP-G_N were also cloned to pPR3N using SfiI. Primers used for cloning are listed in S4 Table.

The MbY2H assays were performed using the manufacturer's instructions with recombinant plasmids that were confirmed by Sanger sequencing. Yeast (NYM51) competent cells were freshly prepared and recombinant bait plasmids, pBT3-SUC-G_N and pBT3-SUC-N were transformed into yeast strain NYM51. Briefly, 1.5µg bait plasmids were added into 100 µl yeast competent cells with 50 µg denatured Yeastmaker Carrier DNA and 500 µl PEG/LiAc. The mixture was incubated at 30ºC for 30 min with mixing every 10 min. Twenty µl DMSO was then added into each reaction, and the cells were incubated at 42ºC for 20 min with mixing every 5 min. After centrifugation at 14,000 rpm for 15 sec, the supernatant was removed, and the pellet was resuspended in 1 ml YPDA media. The re-suspended cells were incubated at 30ºC for 90 min with shaking at 200 rpm. Then, cells were centrifuged at 14,000 rpm for 15 sec, and resuspended in 500 µl sterile 0.9% (w/v) NaCl, which was then spread and cultured on SD/–Trp dropout media at 30ºC until the colonies showed. Several colonies from the same SD/–Trp plate were cultured for preparing yeast competent cells. Then each individual recombinant plasmid, pPR3N-TIP or pPR3N-partial endoCP-G_N (1.5 µg/transformation reaction), was transformed into yeast competent cells

expressing fused Nub-G_N or Nub-N using the same transformation method. The transformants were cultured on both SD/–Leu/–Trp double dropout (DDO) and SD/–Ade/–His/–Leu/–Trp quadruple dropout (QDO) media. The positive controls included transformation of pOst1-NubI into NYM51 that already expressed fused Nub-G_N or Nub-N, as well as co-transformation of pTSU2-APP and pNubG-Fe65 into NYM51. Negative control was transformation of pPR3N (empty vector) into NYM51 that already expressed fused Nub-G_N or Nub-N. All transformants were spread and cultured on both DDO and QDO media at 30ºC incubator. The entire experiment was performed three times.

Yeast β-galactosidase assay

Expression of the reporter gene *LacZ* and the activity of expressed β-galactosidase in yeast cells derived from MbY2H was determined by β-galactosidase assay kit following the manufacturer's protocol (ThermoFisher Scientific). Each yeast colony was transferred and mixed in 250 µl Y-PER by vortex, this initial OD_{660} value was tested. After adding 250 µl 2X β-galactosidase assay buffer to the mixed solution, the reaction was incubated at 37º C until the color change of solution was observed. Two hundred µl of β-galactosidase assay stop solution was added immediately into color change solution, and the reaction time was recorded. Cell debris was removed by centrifugation at 13,000 *g* for 30 seconds. Supernatant was transferred into cuvettes to measure OD_{420} using the blank including 250 µl of Y-PER reagent, 250 µl β-galactosidase assay buffer and 200 µl β-galactosidase assay stop solution. The β-galactosidase activity was calculated using the equation from the manufacturer's protocol.

GFP fusion protein expression and bimolecular fluorescence complementation (BiFC) in *Nicotiana benthamiana*

To visualize protein expression and localization in plants, TSWV structural proteins

(ORFs corresponding to N, G_N, G_NS, G_C and G_CS) and TIP ORFs (mATPase, CP-V, endoCP-V, endoCP-G_N, cyclophilin and enolase) were expressed as fusions to autofluorescent proteins. They were moved from their entry clones into pSITE-2NB (GFP fused to the carboxy terminus of protein of interest) or pSITE-2CA (GFP fused to the amino terminus of the protein of interest) using Gateway LR Clonase [82]. After validation of plasmids by Sanger sequencing, they were transformed into *Agrobacterium tumefaciens* strain LBA 4404. The transformed LBA 4404 was grown for two days at 28ºC and re-suspended in 0.1 M MES and 0.1 M $MgCl_2$ to an OD_{600} between 0.6 to 1. After the addition of 0.1 M acetosyringone, the suspension was incubated at room temperature for two hours, and then infiltrated in transgenic *N. benthamiana* expressing an endoplasmic reticulum (ER) marker fused to red fluorescent protein (m5RFP-HDEL). Two days after infiltration, leaf tissue was mounted in water on a microscope slide for detection of GFP by confocal microscopy. Plants were infiltrated a minimum of two separate occasions with at least two leaves per plant in two plants. A minimum of fifty cells were visualized in each plant to confirm the localization patterns of the proteins *in planta.*

The preliminary localization results and sequence analysis informed the fusion construct design for BiFC assays. Signal peptides were identified in the amino terminus of G_N, G_C, and three TIPs (all cuticle proteins) and the signal peptide is required for proper localization and function of fusion-GFP/YFP proteins in *N. benthamiana* for BiFC assays. Based on the expression and localization results of GFP fusion proteins, we fused half YFPs (either amino or carboxy half of YFP) to the carboxy termini of all proteins with N-terminal signal peptides using BiFC plasmids pSITE-NEN and pSITE-CEN. For TSWV-N - which does not contain a signal peptide and did not show significant differences in localization - the interactions with fusions at both the N- and C- termini of this protein in vectors pSITE-NEN, pSITE-CEN, pSITE-NEC and pSITE-CEC were tested. All ORFS were transferred between plasmids

665 using Gateway LR Clonase II Enzyme Mix (ThermoFisher Scientific) [70]. All clones were
666 transformed into *A. tumefaciens* strain LBA 4404 and confirmed by Sanger sequencing.

667 Each combination of TIPs and TSWV G_N, G_C and N was infiltrated into *N. benthamiana*
668 expressing CFP fused to a nuclear marker, histone 2B, (CFP-H2B), and a minimum of three
669 independent experiments with two plants and two leaves per plant for each combination of
670 proteins. For the analysis of interactions, a minimum of 50 cells with similar localization
671 patterns was required to confirm the interaction and a minimum of two separate images were
672 captured on each occasion for documentation. GST fusions to YFP halves were utilized as a
673 non-binding control for each of the TIPs. To be recorded as a positive interaction,
674 fluorescence of the interacting TSWV protein-TIPs was required to be above that observed
675 between each TIP and GST.

676 **Polyclonal antisera against TIPs**

677 To generate antibodies to the TIPs, the protein sequence was analyzed for multiple
678 features such as antigenicity and hydrophobicity using GenScript protein analysis methods
679 (insert website that contains these bioinformatic tools). For each TIP, a 14 amino acid peptide
680 was selected based on these predictions and by sequence alignments to other predicted
681 protein sequences in GenBank. Due to the conserved CHB4 domain in endoCP-G_N, endoCP-
682 V, and CP-V, the polyclonal antibodies against these three TIPs were generated using their
683 non-conserved region. The peptides were synthesized (GenScript, Piscataway, NJ, United
684 States), and all antisera were produced using mice. The peptide sequences for each TIP that
685 were used for the antibody generation were: cyclophilin, LESFGSHDGKTSKK; enolase,
686 ELRDNDKSQYHGKS; CP-V, TDSGQYRKEKRLED; endoCP-G_N, STKVNPQSFSRSSV;
687 endoCP-V, VNPDGSFQYSYQTG; and mATPase, GHLDKLDPAKITDF.

688 **Immunolabeling thrips guts, Malphigian tubules, and salivary glands**

689 To determine the location of TIPs expression in the most efficient thrips stage that
690 acquires TSWV (L1), we used the TIPs antibodies in immunolocalization experiments.
691 Newly emerged larvae (0-17-hour old) were collected from green beans and were then fed on
692 7% sucrose solution for 3 hours to clean their guts from plant tissues. The larvae were
693 dissected on glass slides using cold phosphate saline (PBS) buffer and Teflon coated razor
694 blades. The dissected thrips were transferred into 2-cm-diam., flat-bottomed watch glasses
695 (U.S. Bureau of Plant Industry, BPI dishes) and the tissues were fixed for 2 hours using 4%
696 paraformaldehyde solution in 50 mM sodium phosphate buffer (pH 7.0). The tissues were
697 washed using PBS buffer after fixation and were incubated with PBS buffer including 1%
698 Triton X-100 overnight. The overnight permeabilized tissues were then washed before
699 incubation in blocking buffer which included PBS, 0.1% Triton X-100 and 10% normal goat
700 serum (NGS) for 1 hour. After removing the blocking buffer, the dissected thrips were
701 incubated with primary antibody, 100 µg/ml mice-generated antisera against each individual
702 TIP (GenScript) that was diluted in antibody buffer (0.1% Triton X-100 and 1% NGS). After
703 wash, 10 µg/ml secondary antibody, goat anti-mouse antibody conjugated with Alexa Fluor
704 488 (ThermoFisher Scientific) was used to incubate the dissected thrips organs. Incubation
705 was performed at room temperature for 2.5 hours, and 1x PBS buffer was used for washing
706 and every wash step included three times, the secondary antibody incubation was protected
707 from light by covering the samples with aluminum foil. After removing antibodies and wash,
708 dissected thrips were incubated for 2 hours with Phalloidin-Alexa 594 conjugated
709 (ThermoFisher Scientific) in 1x PBS with a concentration of 4 units/ml for actin staining.
710 After wash, the tissues were transferred onto glass slides, and SlowFade™ Diamond
711 Antifade Mountant with DAPI (ThermoFisher Scientific) was added onto tissues to stain
712 nuclei. The cover slips were slowly placed on tissues to avoid bubbles, then sealed with

transparent nail polish at edges. After blocking, the dissected thrips tissues that were only incubated with antibody buffer (without adding primary antibody) and the tissues incubated with each pre-immune mouse antiserum (GenScript) were used as controls respectively. All the experiments were performed twice.

Inherent with very small tissues (< 1 mm body size), there were common losses or damaged tissues during the dissection process and staining procedures; so only the number of visibly intact tissue that made it through to microscopic observation were used for data collection and this number varied for each type of tissue (S5 Table). The auto- fluorescent background from thrips tissues incubated with each pre-immune antiserum was slightly higher than the thrips tissues incubated with PBS buffer (no antibody control) (data not shown), therefore, the confocal laser settings (power and percent/gain) were adjusted to remove any background fluorescence observed for these treatments.

Co-localization of TSWV and TIPs in thrips larvae

The two proteins that interacted with G_N in the MbY2H assay, endoCP-G_N and cyclophilin, were used in colocalization experiments to determine if they are expressed in the same midgut cells during virus infection. Synchronized first instar thrips larvae (0-17-hour old) were collected from green beans and were separated into two groups with similar number in each group. Each group of thrips were fed on either healthy (control) or TSWV-symptomatic *E. sonchifolia* leaves (mechanically inoculated) for three acquisition access periods (AAPs) - 24, 48 and 72 hours of exposure - and maintained at 25ºC in an incubator. After each AAP, these larvae were transferred to 7% sucrose for 3 hours to remove the plant tissue from their guts. The thrips were dissected, and tissues were fixed and permeabilized using the same method mentioned above. The overnight permeabilized tissues were sequentially incubated with two primary antibodies at 50 µg/ml, which were rabbit generated anti-G_N (TSWV glycoprotein) and mouse-generated anti-endoCP-G_N/anti-cyclophilin. Then,

738 two secondary antibodies were sequentially used at 10 µg/ml, which were chicken anti-rabbit
739 Alexa Fluor 488, and goat anti-mouse Alexa Fluor 594 (ThermoFisher Scientific). Three
740 wash were performed (1x PBS) between antibodies, all incubations were performed at room
741 temperature for 2.5 hours or at 4ºC overnight, and the secondary antibody incubation was
742 protected from light by covering the samples with aluminum foil. After removal of secondary
743 antibodies, thrips tissues were washed and incubated with Alexa Fluor 647 Phalloidin for
744 actin staining using the same concentration and conditions mentioned above. After three
745 washes with PBS, the tissues were transferred onto glass slides. Nuclei were stained with
746 DAPI and insect tissues were mounted for imaging as described above. The control thrips
747 larvae that fed on healthy *E. sonchifolia* leaves were collected at each time point and were
748 dissected and treated the same as those fed on TSWV-infected leaves. The entire experiment
749 was performed twice.

750 **Laser scanning confocal microscopy**

751 Confocal microscopy was used to detect the GFP produced from expressed TIP-GFP fusions,
752 YFP from interacting TIPs and TSWV structural proteins, localization of TIPs in thrips
753 larvae as well as co-localized TIPs and TSWV. All images were acquired on a Zeiss LSM
754 780 laser scanning confocal microscope using the C-Apochromat 40x/1.2 W Korr M27 and
755 Plan-Apochromat 20x/0.8 M27 objectives. Image acquisition was conducted on Zen 2 black
756 edition v. 10.0.0 at 1024 x 1024 pixels with a scan rate of 1.58µs per pixel with pixel average
757 of 4 bit and 16 bit depth. The laser power percent/gain settings for detection of nuclei and
758 actin as well as bright field were adjusted accordingly. Laser power percent/gain settings for
759 detection of TIPs and TSWV were equal or smaller than their controls. Z-stacks were taken
760 for localization of TIPs in thrips, and co-localization of TIPs and TSWV respectively. Eight
761 (TIPs localization) and ten (co-localization) Z-stack slides were processed using Maximum

762 intensity projection using Zen 2 black. Zen 2 blue edition lite 2010 v. 2.0.0.0 was used for
763 image conversion to jpeg format.
764
765 **Acknowledgements:** This project was supported by the following grants: USDA-NIFA
766 2007-35319-18326 and 2016-67013-27492, USDA-FNRI 6034-22000-039-06S, and
767 National Science Foundation CAREER Grant IOS-0953786. Ismael Badillo Vargas was
768 partially supported by the National Institute of Food and Agriculture Predoctoral Fellowship,
769 grant KS602489. We thank Thomas L. German and Ranjit Dasgupta for providing purified
770 G_N for protein overlays.

771 **References**

772 1. Gubler DJ. Resurgent vector-borne diseases as a global health problem. Emerg Infect
773 Dis. 1998;4: 442-50. doi: 10.3201/eid0403.980326. PubMed PMID: 9716967; PubMed
774 Central PMCID: PMC2640300.
775 2. Gubler DJ. The global emergence/resurgence of arboviral diseases as public health
776 problems. Arch Med Res. 2002;33: 330-42. doi:10.1016/S0188-4409(02)00378-8. PubMed
777 PMID: 12234522.
778 3. Elliott RM. Emerging viruses: the Bunyaviridae. Mol Med. 1997;3: 572-7. PubMed
779 PMID: 9323708; PubMed Central PMCID: PMC2230091.
780 4. Horne KM, Vanlandingham DL. Bunyavirus-vector interactions. Viruses. 2014;6:
781 4373-97. doi: 10.3390/v6114373. PubMed PMID: 25402172; PubMed Central PMCID:
782 PMC4246228.
783 5. Beaty BJ, Bishop DH. Bunyavirus-vector interactions. Virus Res. 1988;10: 289-301.
784 doi: 10.1016/0168-1702(88)90071-8. PubMed PMID: 3046165.
785 6. Rotenberg D, Jacobson AL, Schneweis DJ, Whitfield AE. Thrips transmission of

786 tospoviruses. Curr Opin Virol. 2015;15: 80-9. doi: 10.1016/j.coviro.2015.08.003. PubMed
787 PMID: 26340723.
788 7. Whitfield AE, Ullman DE, German TL. Tospovirus-thrips interactions. Annu Rev
789 Phytopathol. 2005;43: 459-89. doi: 10.1146/annurev.phyto.43.040204.140017. PubMed
790 PMID: 16078892.
791 8. Parrella G, Gognalons P, Gebre-Selassie K, Vovlas C, Marchoux G. An update of the
792 host range of Tomato spotted wilt virus. J Plant Pathol. 2003;85: 227-64.
793 9. Montero-Astua M, Rotenberg D, Leach-Kieffaber A, Schneweis BA, Park S, Park JK,
794 et al. Disruption of vector transmission by a plant-expressed viral glycoprotein. Mol Plant
795 Microbe Interact. 2014;27: 296-304. doi: 10.1094/MPMI-09-13-0287-FI. PubMed PMID:
796 24405031.
797 10. Whitfield AE, Kumar NK, Rotenberg D, Ullman DE, Wyman EA, Zietlow C, et al. A
798 soluble form of the *tomato spotted wilt virus* (TSWV) glycoprotein GN (GN-S) inhibits
799 transmission of TSWV by *Frankliniella occidentalis*. Phytopathology. 2008;98(1):45-50.
800 Epub 2008/10/24. doi: 10.1094/PHYTO-98-1-0045. PubMed PMID: 18943237.
801 11. Whitfield AE, Ullman DE, German TL. Expression and characterization of a soluble
802 form of tomato spotted wilt virus glycoprotein G_N. J Virol. 2004;78: 13197-206. doi:
803 10.1128/JVI.78.23.13197-13206.2004. PubMed PMID: 15542672; PubMed Central PMCID:
804 PMC524983.
805 12. de Haan P, Kormelink R, de Oliveira Resende R, van Poelwijk F, Peters D, Goldbach
806 R. Tomato spotted wilt virus L RNA encodes a putative RNA polymerase. J Gen Virol.
807 1991;72: 2207-16. doi: 10.1099/0022-1317-72-9-2207. PubMed PMID: 1895058.
808 13. Kormelink R, de Haan P, Meurs C, Peters D, Goldbach R. The nucleotide sequence of
809 the M RNA segment of tomato spotted wilt virus, a bunyavirus with two ambisense RNA
810 segments. J Gen Virol. 1992;73: 2795-804. doi: 10.1099/0022-1317-73-11-2795. PubMed

811 PMID: 1431808.

812 14. Lewandowski DJ, Adkins S. The tubule-forming NSm protein from Tomato spotted
813 wilt virus complements cell-to-cell and long-distance movement of Tobacco mosaic virus
814 hybrids. Virology. 2005;342: 26-37. doi: 10.1016/j.virol.2005.06.050. PubMed PMID:
815 16112159.

816 15. Soellick T, Uhrig JF, Bucher GL, Kellmann JW, Schreier PH. The movement protein
817 NSm of tomato spotted wilt tospovirus (TSWV): RNA binding, interaction with the TSWV N
818 protein, and identification of interacting plant proteins. Proc Natl Acad Sci USA. 2000;97:
819 2373-8. doi: 10.1073/pnas.030548397. PubMed PMID: 10688879; PubMed Central PMCID:
820 PMC15808.

821 16. Storms MM, Kormelink R, Peters D, Van Lent JW, Goldbach RW. The nonstructural
822 NSm protein of tomato spotted wilt virus induces tubular structures in plant and insect cells.
823 Virology. 1995;214: 485-93. doi: 10.1006/viro.1995.0059. PubMed PMID: 8553550.

824 17. de Haan P, Wagemakers L, Peters D, Goldbach R. The S RNA segment of tomato
825 spotted wilt virus has an ambisense character. J Gen Virol. 1990;71: 1001-7.
826 doi:10.1099/0022-1317-71-5-1001. PubMed PMID: 1693160.

827 18. de Ronde D, Pasquier A, Ying S, Butterbach P, Lohuis D, Kormelink R. Analysis of
828 Tomato spotted wilt virus NSs protein indicates the importance of the N-terminal domain for
829 avirulence and RNA silencing suppression. Mol Plant Pathol. 2014;15: 185-95. doi:
830 10.1111/mpp.12082. PubMed PMID: 24103150.

831 19. Margaria P, Bosco L, Vallino M, Ciuffo M, Mautino GC, Tavella L, et al. The NSs
832 protein of tomato spotted wilt virus is required for persistent infection and transmission by
833 Frankliniella occidentalis. J Virol. 2014;88: 5788-802. doi: 10.1128/JVI.00079-14. PubMed
834 PMID: 24623427; PubMed Central PMCID: PMC4019118.

835 20. Takeda A, Sugiyama K, Nagano H, Mori M, Kaido M, Mise K, et al. Identification of
836 a novel RNA silencing suppressor, NSs protein of Tomato spotted wilt virus. FEBS Lett.
837 2002;532: 75-9. doi:10.1016/S0014-5793(02)03632-3. PubMed PMID: 12459466.
838 21. Ullman DE, German TL, Sherwood JL, Westcot DM, Cantone FA. Tospovirus
839 replication in insect vector cells: immunocytochemical evidence that the nonstructural protein
840 encoded by the S RNA of tomato spotted wilt tospovirus is present in thrips vector cells.
841 Phytopathology. 1993;83: 456-63. doi:10.1094/Phyto-83-456.
842 22. Wijkamp I, van Lent J, Kormelink R, Goldbach R, Peters D. Multiplication of tomato
843 spotted wilt virus in its insect vector, *Frankliniella occidentalis*. J Gen Virol. 1993;74: 341-9.
844 doi: 10.1099/0022-1317-74-3-341. PubMed PMID: 8445364.
845 23. Nagata T, Inoue-Nagata AK, Smid HM, Goldbach R, Peters D. Tissue tropism related
846 to vector competence of Frankliniella occidentalis for tomato spotted wilt tospovirus. J Gen
847 Virol.. 1999;80: 507-15. doi: 10.1099/0022-1317-80-2-507. PubMed PMID: 10073714.
848 24. Ullman DE, Cho JJ, Mau RFL, Westcot DM, Custer DM. A midgut barrier to tomato
849 spotted wilt virus acquisition by adult western flower thrips. Phytopathology. 1992;82: 1333-
850 42. doi:10.1094/Phyto-82-1333.
851 25. Sin SH, McNulty BC, Kennedy GG, Moyer JW. Viral genetic determinants for thrips
852 transmission of Tomato spotted wilt virus. Proc Natl Acad Sci USA. 2005;102: 5168-73. doi:
853 10.1073/pnas.0407354102. PubMed PMID: 15753307; PubMed Central PMCID:
854 PMC552972.
855 26. Rebers JE, Riddiford LM. Structure and expression of a Manduca sexta larval cuticle
856 gene homologous to Drosophila cuticle genes. J Mol Biol. 1988;203: 411-23.
857 doi:10.1016/0022-2836(88)90009-5. PubMed PMID: 2462055.
858 27. Schneweis DJ, Whitfield AE, Rotenberg D. Thrips developmental stage-specific
859 transcriptome response to tomato spotted wilt virus during the virus infection cycle in

Frankliniella occidentalis, the primary vector. Virology. 2017;500: 226-37. doi: 10.1016/j.virol.2016.10.009. PubMed PMID: 27835811.

28. Liu W, Gray S, Huo Y, Li L, Wei T, Wang X. Proteomic analysis of interaction between a plant virus and its vector insect reveals new functions of hemipteran cuticular protein. Mol Cell Proteomics. 2015;14: 2229-42. doi: 10.1074/mcp.M114.046763. PubMed PMID: 26091699; PubMed Central PMCID: PMC4528249.

29. Montero-Astua M, Ullman DE, Whitfield AE. Salivary gland morphology, tissue tropism and the progression of tospovirus infection in *Frankliniella occidentalis*. Virology. 2016;493: 39-51. doi: 10.1016/j.virol.2016.03.003. PubMed PMID: 26999025.

30. Elliott RM, Schmaljohn CS. Bunyaviridae. In: Knipe DM, Howley PM, editors. Fields Virology. Philadelphia, PA: Lippincott Williams & Wilkins; 2013.

31. Wang H, Alminaite A, Vaheri A, Plyusnin A. Interaction between hantaviral nucleocapsid protein and the cytoplasmic tail of surface glycoprotein Gn. Virus Res. 2010;151: 205-12. doi: 10.1016/j.virusres.2010.05.008. PubMed PMID: 20566401.

32. Ribeiro D, Borst JW, Goldbach R, Kormelink R. Tomato spotted wilt virus nucleocapsid protein interacts with both viral glycoproteins Gn and Gc in planta. Virology. 2009;383: 121-30. doi: 10.1016/j.virol.2008.09.028. PubMed PMID: 18973913.

33. Richmond KE, Chenault K, Sherwood JL, German TL. Characterization of the nucleic acid binding properties of tomato spotted wilt virus nucleocapsid protein. Virology. 1998;248: 6-11. doi: 10.1006/viro.1998.9223. PubMed PMID: 9705250.

34. Andersen SO, Hojrup P, Roepstorff P. Insect cuticular proteins. Insect Biochem Mol Biol. 1995;25: 153-76. PubMed PMID: 7711748.

35. Willis JH. Structural cuticular proteins from arthropods: annotation, nomenclature, and sequence characteristics in the genomics era. Insect Biochem Mol Biol. 2010;40: 189-204. doi: 10.1016/j.ibmb.2010.02.001. PubMed PMID: 20171281; PubMed Central PMCID:

885 PMCPMC2872936.

886 36. Chapman RF, Simpson SJ, Douglas AE. The Insects: Structure and Function. 5th ed.
887 Cambridge: Cambridge University Press; 2013.

888 37. Maddrell SHP, Gardiner BOC. The permeability of the cuticular lining of the insect
889 alimentary canal. J Exp Biol. 1980;85: 227-37.

890 38. Ullman DE, Westcot DM, Hunter WB, Mau RFL. Internal anatomy and morphology
891 of *Frankliniella occidentalis* (Pergande) (Thysanoptera: Thripidae) with special reference to
892 interactions between thrips and tomato spotted wilt virus. Int J Insect Morphol. 1989;18: 289-
893 310. doi: 10.1016/0020-7322(89)90011-1.

894 39. Zhu KY, Merzendorfer H, Zhang W, Zhang J, Muthukrishnan S. Biosynthesis,
895 Turnover, and Functions of Chitin in Insects. Annu Rev Entomol. 2016;61: 177-96. doi:
896 10.1146/annurev-ento-010715-023933. PubMed PMID: 26982439.

897 40. Cristofoletti PT, Ribeiro AF, Deraison C, Rahbe Y, Terra WR. Midgut adaptation and
898 digestive enzyme distribution in a phloem feeding insect, the pea aphid *Acyrthosiphon pisum*.
899 J Insect Physiol. 2003;49: 11-24. doi: 10.1016/S0022-1910(02)00222-6. PubMed PMID:
900 12770012.

901 41. Silva CP, Silva JR, Vasconcelos FF, Petretski MD, Damatta RA, Ribeiro AF, et al.
902 Occurrence of midgut perimicrovillar membranes in paraneopteran insect orders with
903 comments on their function and evolutionary significance. Arthropod Struct Dev. 2004;33:
904 139-48. doi: 10.1016/j.asd.2003.12.002. PubMed PMID: 18089029.

905 42. Albuquerque-Cunha JM, Gonzalez MS, Garcia ES, Mello CB, Azambuja P, Almeida
906 JC, et al. Cytochemical characterization of microvillar and perimicrovillar membranes in the
907 posterior midgut epithelium of Rhodnius prolixus. Arthropod Struct Dev. 2009;38: 31-44.
908 doi: 10.1016/j.asd.2008.06.001. PubMed PMID: 18602023.

909 43. Terra WR, Costa RH, Ferreira C. Plasma membranes from insect midgut cells. An

910 Acad Bras Cienc. 2006;78: 255-69. doi: /S0001-37652006000200007. PubMed PMID:
911 16710565.
912 44. Alvarenga ES, Mansur JF, Justi SA, Figueira-Mansur J, Dos Santos VM, Lopez SG,
913 et al. Chitin is a component of the *Rhodnius prolixus* midgut. Insect Biochem Mol Biol.
914 2016;69: 61-70. doi: 10.1016/j.ibmb.2015.04.003. PubMed PMID: 25910679.
915 45. Wang H, Wu K, Liu Y, Wu Y, Wang X. Integrative proteomics to understand the
916 transmission mechanism of *Barley yellow dwarf virus-GPV* by its insect vector
917 *Rhopalosiphum padi*. Sci Rep. 2015;5: 10971. doi: 10.1038/srep10971. PubMed PMID:
918 26161807; PubMed Central PMCID: PMC4498328.
919 46. Kumari S, Roy S, Singh P, Singla-Pareek SL, Pareek A. Cyclophilins: proteins in
920 search of function. Plant Signal Behav. 2013;8: e22734. doi: 10.4161/psb.22734. PubMed
921 PMID: 23123451; PubMed Central PMCID: PMC3745578.
922 47. von Hahn T, Ciesek S. Cyclophilin polymorphism and virus infection. Curr Opin
923 Virol. 2015;14: 47-9. doi: 10.1016/j.coviro.2015.07.012. PubMed PMID: 26281011.
924 48. Liu H, Xue Q, Cao W, Yang F, Ma L, Liu W, et al. Foot-and-mouth disease virus
925 nonstructural protein 2B interacts with cyclophilin A, modulating virus replication. FASEB J.
926 2018; 15: fj201701351. doi: 10.1096/fj.201701351. PubMed PMID: 29906248.
927 49. Kovalev N, Nagy PD. Cyclophilin A binds to the viral RNA and replication proteins,
928 resulting in inhibition of tombusviral replicase assembly. J Virol. 2013;87: 13330-42. doi:
929 10.1128/JVI.02101-13. PubMed PMID: 24089553; PubMed Central PMCID: PMC3838255.
930 50. Tamborindeguy C, Bereman MS, DeBlasio S, Igwe D, Smith DM, White F, et al.
931 Genomic and proteomic analysis of *Schizaphis graminum* reveals cyclophilin proteins are
932 involved in the transmission of *cereal yellow dwarf virus*. Plos One. 2013;8: e71620. doi:
933 10.1371/journal.pone.0071620. PubMed PMID: 23951206; PubMed Central PMCID:
934 PMC3739738.

935 51. Yang X, Thannhauser TW, Burrows M, Cox-Foster D, Gildow FE, Gray SM.
936 Coupling genetics and proteomics to identify aphid proteins associated with vector-specific
937 transmission of polerovirus (luteoviridae). J Virol. 2008;82: 291-9. doi: 10.1128/JVI.01736-
938 07. PubMed PMID: 17959668; PubMed Central PMCID: PMC2224398.
939 52. Badillo-Vargas IE, Rotenberg D, Schneweis DJ, Hiromasa Y, Tomich JM, Whitfield
940 AE. Proteomic analysis of *Frankliniella occidentalis* and differentially expressed proteins in
941 response to *tomato spotted wilt virus* infection. J Virol. 2012;86: 8793-809. doi:
942 10.1128/JVI.00285-12. PubMed PMID: 22696645; PubMed Central PMCID: PMC3421711.
943 53. An P, Wang LH, Hutcheson-Dilks H, Nelson G, Donfield S, Goedert JJ, et al.
944 Regulatory polymorphisms in the cyclophilin A gene, PPIA, accelerate progression to AIDS.
945 PLoS Pathog. 2007;3: e88. doi: 10.1371/journal.ppat.0030088. PubMed PMID: 17590083;
946 PubMed Central PMCID: PMCPMC1894826.
947 54. Bleiber G, May M, Martinez R, Meylan P, Ott J, Beckmann JS, et al. Use of a
948 combined ex vivo/in vivo population approach for screening of human genes involved in the
949 human immunodeficiency virus type 1 life cycle for variants influencing disease progression.
950 J Virol. 2005;79: 12674-80. doi: 10.1128/JVI.79.20.12674-12680.2005. PubMed PMID:
951 16188970. PubMed Central PMCID: PMC1235818.
952 55. Chatterji U, Bobardt M, Selvarajah S, Yang F, Tang H, Sakamoto N, et al. The
953 isomerase active site of cyclophilin A is critical for hepatitis C virus replication. J Biol Chem.
954 2009;284: 16998-7005. doi: 10.1074/jbc.M109.007625. PubMed PMID: 19380579. PubMed
955 Central PMCID: PMC2719337.
956 56. Kaul A, Stauffer S, Berger C, Pertel T, Schmitt J, Kallis S, et al. Essential role of
957 cyclophilin A for hepatitis C virus replication and virus production and possible link to
958 polyprotein cleavage kinetics. PLoS Pathog. 2009;5: e1000546. doi:
959 10.1371/journal.ppat.1000546. PubMed PMID: 19680534; PubMed Central PMCID:

960 PMCPMC2718831.

961 57. Rits MAN, van Dort KA, Kootstra NA. Polymorphisms in the regulatory region of the

962 Cyclophilin A gene influence the susceptibility for HIV-1 infection. Plos One. 2008;3: e3975.

963 doi: 10.1371/journal.pone.0003975. PubMed PMID: 19092998; PubMed Central PMCID:

964 PMCPMC2599883.

965 58. Yang F, Robotham JM, Nelson HB, Irsigler A, Kenworthy R, Tang H. Cyclophilin A

966 is an essential cofactor for hepatitis C virus infection and the principal mediator of

967 cyclosporine resistance in vitro. J Virol. 2008;82: 5269-78. doi: 10.1128/JVI.02614-07.

968 PubMed PMID: 18385230. PubMed Central PMCID: PMC2395199.

969 59. Krupovic M, Koonin EV. Multiple origins of viral capsid proteins from cellular

970 ancestors. Proc Natl Acad Sci USA. 2017;114: E2401-E10. doi: 10.1073/pnas.1621061114.

971 PubMed PMID: 28265094; PubMed Central PMCID: PMCPMC5373398.

972 60. Brown JR, Doolittle WF. Archaea and the prokaryote-to-eukaryote transition.

973 Microbiol Mol Biol Rev. 1997;61: 456-502. PubMed PMID: PMC232621. PubMed Central

974 PMCID: PMC232621.

975 61. Van Lint P, Libert C. Chemokine and cytokine processing by matrix

976 metalloproteinases and its effect on leukocyte migration and inflammation. J Leukoc Biol.

977 2007;82: 1375-81. doi: 10.1189/jlb.0607338. PubMed PMID: 17709402.

978 62. Zhang F, Guo H, Zheng H, Zhou T, Zhou Y, Wang S, et al. Massively parallel

979 pyrosequencing-based transcriptome analyses of small brown planthopper (*Laodelphax*

980 *striatellus*), a vector insect transmitting rice stripe virus (RSV). BMC Genomics. 2010;11:

981 303. doi: 10.1186/1471-2164-11-303. PubMed PMID: 20462456; PubMed Central PMCID:

982 PMCPMC2885366.

983 63. Munoz Mde L, Limon-Camacho G, Tovar R, Diaz-Badillo A, Mendoza-Hernandez G,

984 Black WCt. Proteomic identification of dengue virus binding proteins in *Aedes aegypti*

985 mosquitoes and *Aedes albopictus* cells. Biomed Res Int. 2013;2013: 875958. doi:
986 10.1155/2013/875958. PubMed PMID: 24324976; PubMed Central PMCID:
987 PMCPMC3842078.
988 64. Colpitts TM, Cox J, Nguyen A, Feitosa F, Krishnan MN, Fikrig E. Use of a tandem
989 affinity purification assay to detect interactions between West Nile and dengue viral proteins
990 and proteins of the mosquito vector. Virology. 2011;417: 179-87. doi:
991 10.1016/j.virol.2011.06.002. PubMed PMID: PMC3166580.
992 65. Popova-Butler A, Dean DH. Proteomic analysis of the mosquito *Aedes aegypti*
993 midgut brush border membrane vesicles. J Insect Physiol. 2009;55: 264-72. doi:
994 10.1016/j.jinsphys.2008.12.008. PubMed PMID: 19133270; PubMed Central PMCID:
995 PMCPMC2735124.
996 66. Means JC, Passarelli AL. Viral fibroblast growth factor, matrix metalloproteases, and
997 caspases are associated with enhancing systemic infection by baculoviruses. Proc Natl Acad
998 Sci USA. 2010;107: 9825-30. doi: 10.1073/pnas.0913582107. PubMed PMID: 20457917;
999 PubMed Central PMCID: PMCPMC2906863.
1000 67. Rojo G, Chamorro M, Salas ML, Vinuela E, Cuezva JM, Salas J. Migration of
1001 mitochondria to viral assembly sites in African swine fever virus-infected cells. J Virol.
1002 1998;72: 7583-8. PubMed PMID: 9696857; PubMed Central PMCID: PMCPMC110008.
1003 68. Bandla MD, Campbell LR, Ullman DE, Sherwood JL. Interaction of tomato spotted
1004 wilt tospovirus (TSWV) glycoproteins with a thrips midgut protein, a potential cellular
1005 receptor for TSWV. Phytopathology. 1998;88: 98-104. doi: 10.1094/PHYTO.1998.88.2.98.
1006 PubMed PMID: 18944977.
1007 69. Bautista RC, Mau RFL, Cho JJ, Custer DM. Potential of tomato spotted wilt
1008 tospovirus plant hosts in Hawaii as virus reservoirs for transmission by *Frankliniella*
1009 *occidentalis* (Thysanoptera: Thripidae). Phytopathology. 1995;85: 953-8. doi: 10.1094/Phyto-

1010 85-953.

1011 70. Martin K, Kopperud K, Chakrabarty R, Banerjee R, Brooks R, Goodin MM. Transient
1012 expression in *Nicotiana benthamiana* fluorescent marker lines provides enhanced definition
1013 of protein localization, movement and interactions *in planta*. Plant J. 2009;59: 150-62. doi:
1014 10.1111/j.1365-313X.2009.03850.x. PubMed PMID: 19309457.

1015 71. Cilia M, Fish T, Yang X, McLaughlin M, Thannhauser TW, Gray S. A comparison of
1016 protein extraction methods suitable for gel-based proteomic studies of aphid proteins. J
1017 Biomol Tech. 2009;20: 201-15. PubMed PMID: 19721822; PubMed Central PMCID:
1018 PMC2729484.

1019 72. Cilia M, Tamborindeguy C, Fish T, Howe K, Thannhauser TW, Gray S. Genetics
1020 coupled to quantitative intact proteomics links heritable aphid and endosymbiont protein
1021 expression to circulative polerovirus transmission. J Virol. 2011;85: 2148-66. doi:
1022 10.1128/JVI.01504-10. PubMed PMID: 21159868; PubMed Central PMCID: PMC3067806.

1023 73. Dobson L, Remenyi I, Tusnady GE. CCTOP: a consensus constrained TOPology
1024 prediction web server. Nucleic Acids Res. 2015;43: W408-12. doi: 10.1093/nar/gkv451.
1025 PubMed PMID: 25943549; PubMed Central PMCID: PMCPMC4489262.

1026 74. Nielsen H. Predicting secretory proteins with SignalP. Methods Mol Biol.
1027 2017;1611:59-73. doi: 10.1007/978-1-4939-7015-5_6. PubMed PMID: 28451972.

1028 75. Ioannidou ZS, Theodoropoulou MC, Papandreou NC, Willis JH, Hamodrakas SJ.
1029 CutProtFam-Pred: detection and classification of putative structural cuticular proteins from
1030 sequence alone, based on profile hidden Markov models. Insect Biochem Mol Biol. 2014;52:
1031 51-9. doi: 10.1016/j.ibmb.2014.06.004. PubMed PMID: 24978609; PubMed Central PMCID:
1032 PMCPMC4143468.

1033 76. Magkrioti CK, Spyropoulos IC, Iconomidou VA, Willis JH, Hamodrakas SJ.
1034 cuticleDB: a relational database of Arthropod cuticular proteins. BMC Bioinformatics.

2004;5: 138. doi: 10.1186/1471-2105-5-138. PubMed PMID: 15453918; PubMed Central PMCID: PMCPMC522807.

77. Kumar S, Stecher G, Tamura K. MEGA7: molecular evolutionary genetics analysis version 7.0 for bigger datasets. Mol Biol Evol. 2016;33: 1870-4. doi: 10.1093/molbev/msw054. PubMed PMID: 27004904.

78. Schwarz R, Dayhoff M. Matrices for detecting distant relationships. In: Dayhoff M, editor. Atlas of protein sequences: National Biomedical Research Foundation; 1979. p. 353-8.

79. Jones DT, Taylor WR, Thornton JM. The rapid generation of mutation data matrices from protein sequences. Comput Appl Biosci. 1992;8: 275-82. PubMed PMID: 1633570.

80. Kim JW. Disease resistance in tobacco and tomato plants transformed with the Tomato spotted wilt virus nucleocapsid gene. Plant Dis. 1994;78: 615-21. doi: 10.1094/PD-78-0615.

81. Adkins S, Choi TJ, Israel BA, Bandla MD, Richmond KE, Schultz KT, et al. Baculovirus expression and processing of tomato spotted wilted tospovirus glycoproteins. Phytopathology. 1996;86: 849-55. doi: 10.1094/Phyto-86-849.

82. Chakrabarty R, Banerjee R, Chung SM, Farman M, Citovsky V, Hogenhout SA, et al. PSITE vectors for stable integration or transient expression of autofluorescent protein fusions in plants: probing *Nicotiana benthamiana*-virus interactions. Mol Plant Microbe Interact. 2007;20: 740-50. doi: 10.1094/MPMI-20-7-0740. PubMed PMID: 17601162.

Figure Legends

Fig 1. Overlay assay using purified virions and *F. occidentalis* first instar proteins resolved in two-dimensional gels.

Total proteins (150 µg) extracted from pooled healthy first instar larvae (0-17-hour old) of *F. occidentalis* were resolved by 2-D gel electrophoresis and transferred to nitrocellulose membranes that were used for virus overlay assays. After blocking, membranes were incubated overnight with purified TSWV at 25 µg/mL (B) or blocking buffer (A) (negative control) respectively and then incubated with polyclonal rabbit anti-TSWV G_N antiserum. Only protein spots that consistently bound to purified TSWV in three (spots 1, 2, 4, 6, and 7) and four (spots 3, 5, and 8) replicates of the virus overlay assay were collected from three individual picking gels and subjected to ESI mass spectrometry for protein identification. Protein spots observed in the no overlay control membrane represent non-specific binding and were not collected for further analysis. Molecular mass (in kilodaltons) is shown on the Y axis and pI (as pH range) is shown on the X axis.

Fig 2. Overlay assay using recombinant G_N and *F. occidentalis* first instar proteins resolved in two-dimensional gels.

150 µg total proteins extracted from pooled healthy first instar larvae (0-17-hour old) of *F. occidentalis* were resolved by 2-D gel electrophoresis and transferred to nitrocellulose membranes that were used for overlay assays. The membranes were incubated overnight with recombinant TSWV G_N (3.5 µg/mL) (B) or blocking buffer (A). Using the polyclonal rabbit anti-TSWV G_N, protein spots that consistently bound to the recombinant TSWV G_N in two (spots 1 through 11) replicates of the overlay assay were collected from two individual picking gels and subjected to ESI mass spectrometry for protein identification. Protein spots observed in the no overlay control membrane represent non-specific binding and were not collected for further analysis. Molecular mass (in kilodaltons) is shown on the Y axis and pI (as pH range) is shown on the X axis.

Fig 3. Validation of TSWV N/G_N-TIPs and G_N-partial endoCP-G_N using split-ubiquitin membrane-based yeast two hybrid (MbY2H). (A) Interactions between TSWV N, (B) G_N and six TIPs. TSWV N and G_N were expressed as N/G_N-Cub, and TIPs were expressed as NubG-TIPs using MbY2H vectors. (C) Interactions between TSWV G_N and different regions of endoCP-G_N. EndoCP-G_N was expressed as either the N-terminal domain (amino acids 1-176 and 1-189) that includes the non-conserved region or the C-terminal region (amino acids 177-284 and 190-284) that includes the conserved Chitin_bind_4 motif (CHB4) of endoCP-G_N. Interactions between TSWV proteins and NubI or NubG were used as positive and negative controls respectively. Co-transformation of pTSU2-APP and pNubG-Fe65 into NYM51 was used as another positive control (data not shown). DDO represents yeast double dropout (SD/-Leu/-Trp) media, and QDO represents yeast quadruple dropout (SD/-Ade/-His/-Leu/-Trp) media.

Fig 4. Confirmation of interactions between TSWV proteins and TIPs using bimolecular fluorescence complementation (BiFC) in *N. benthamiana.* Plants transgenic for a nuclear marker fused to CFP, CFP-H2B, were infiltrated with suspensions of TIPs proteins fused to either the amino or carboxy terminus of YFP. The interactions that tested positive as seen by fluorescence of YFP are indicated in the BiFC column. The CFP-H2B column is indicated to give cellular reference and the overlay between the two is also shown. The final column is the nucleus enlarged to show detail of the interacting TIPs with cellular context. One infiltration with a TIP and glutathione S-transferase is included as a representative of a non-binding control image. All scale bars are equal to 20 μM.

Fig 5. Immunolabeling of TIPs within first instar larvae of *F. occidentalis*. The synchronized first instar larvae (0-17-hour old) were kept on 7% sucrose solution for 3 hours

to clean their guts from plant tissues. These larvae were then dissected and immunolabeled using specific antibodies against each TIP as indicated. Thrips tissues incubated with pre-immune mouse serum are depicted here. Confocal microscopy detected the green fluorescence (Alexa Fluor 488) that represents the localization of each TIP. TIPs were mainly localized at foregut (FG), midgut (MG) that include epithelial cells and visceral muscle (VM), principle salivary glands (PSG), tubular salivary glands (TSG), and Malpighian tubules (MT). All scale bars are equal to 50 μM.

Fig 6. Co-localization of TSWV (G_N) and endoCP-G_N or cyclophilin within *F. occidentalis*. The synchronized first instar larvae (0-17-hour old) were fed on TSWV symptomatic or healthy *E. sonchifolia* leaves for 24, 48 and 72 hours. At each time point, thrips larvae were collected and kept on 7% sucrose solution for 3 hours before dissection. Specific antibodies against TSWV (G_N), endoCP-G_N and cyclophilin were used to label virus and TIPs. Alexa Fluor 488 (green) labeled TSWV (G_N) that represents the localization of TSWV (G_N) and Alexa Fluor 594 (red) labeled endoCP-G_N and cyclophilin, which represent the localization of TIPs. Thrips that fed on healthy *E. sonchifolia* leaves were used as control, in which green fluorescence was not detected and signal from these insects were used to adjust confocal microscope settings to remove background fluorescence. TIPs and TSWV were co-localized at anterior midgut (MG1) that include epithelial cells and visceral muscle (VM) (from 24h to 72h). FG, foregut; PSG, principle salivary glands; TSG, tubular salivary glands. All scale bars are equal to 50 μM.

Supporting Information

S1 Fig. Phylogenetic analysis of CP R&R consensus sequences in first instar larvae of *F. occidentalis*. The Neighbor-Joining (NJ) method was performed with the Jones Taylor Thorton (JTT) matrix-based method for amino acid substitutions with Gamma distribution to model the variation among sites. The bootstrap consensus tree (500 replicates) was generated by the NJ algorithm with pairwise deletion for handling gaps. Branches corresponding to partitions reproduced in less than 70% bootstrap replicates were collapsed. The numbers shown next to branches indicate the percentage of replicate trees in which the associated taxa (sequences) clustered together in the bootstrap test. The analysis involved 46 sequences – the three cuticular TSWV-interacting proteins (TIPs: cuticle protein-V (CP-V), endocuticle structural glycoprotein-V (endoCP-V) and endocuticle structural glycoprotein-G_N (endoCP-G_N) (blue text), the 'gold-standard' Pfam database extended R&R consensus sequence (pf00379), 19 insect orthologous sequences obtained from NCBI GenBank, and 23 structural CPs and endoCPs (translated transcripts, designated with FOCC or CUFF identifiers) previously reported to be differentially-expressed in TSWV-infected L1s of *F. occidentalis* (27). There were 95 amino-acid positions in the final dataset. RR1 and RR2 = Cuticle Protein Rebers and Riddiford (CPR family, RR1 and RR2 types) extended consensus, a conserved chitin-binding motif (chitin_bind_4 = CHB4).

S2 Fig. Localization in *N. benthamiana* of TIPs fused green fluorescent protein (GFP). *N. benthamiana* transgenic for an RFP-ER marker were infiltrated with *Agrobacterium tumefaciens* strain LBA 4404 suspensions of TIPs constructs. Each row indicates the specific TIP-GFP fusion in relation to the RFP-ER marker. The columns are as follows: GFP channel, RFP channel and the overlay between the two channels. All scale bars are equal to 20 μM.

S3 Fig. Individual channels of immune-labeled TIPs within first instar larvae of *F. occidentalis*. The synchronized first instar larvae (0-17-hour old) were dissected and immunolabeled using specific antibodies against each TIP as indicated. Thrips tissues incubated with pre-immune mouse antiserum as controls are depicted here. Confocal microscopy detected green fluorescence (Alexa Fluor 488) that represents the localization of each TIP, red represents Alexa Fluor 594 labeled actin; blue represents DAPI labeled nuclei. All scale bars are equal to 50 μM.

S4 Fig. Individual channels of immunolabeled thrips that were fed on TSWV or healthy *E. sonchifolia*. The synchronized first instar larvae (0-17-hour old) were fed on TSWV symptomatic or healthy *E. sonchifolia* leaves for 24, 48 and 72 hours. Plant tissues were removed and thrips alimentary canals were cleared, dissected and incubated with antisera against cyclophilin, endoCP-G_N and TSWV (G_N) as indicated. Red, Alexa Fluor 594 labeled TIPs; green, Alexa Fluor 488 labeled TSWV (G_N), purple, Alexa Fluor 594 labeled actin; blue, DAPI labeled nuclei.

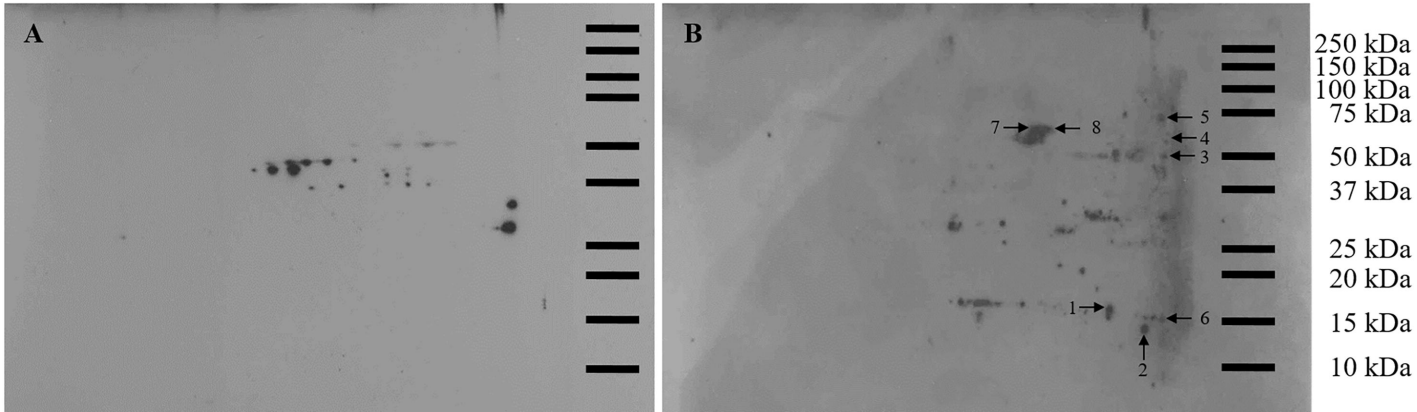
10
pH
3
A
10
pH
3
B
250 kDa
150 kDa
100 kDa
75 kDa
50 kDa
37 kDa
25 kDa
20 kDa
15 kDa
10 kDa
1
2
3
4
5
6
7
8

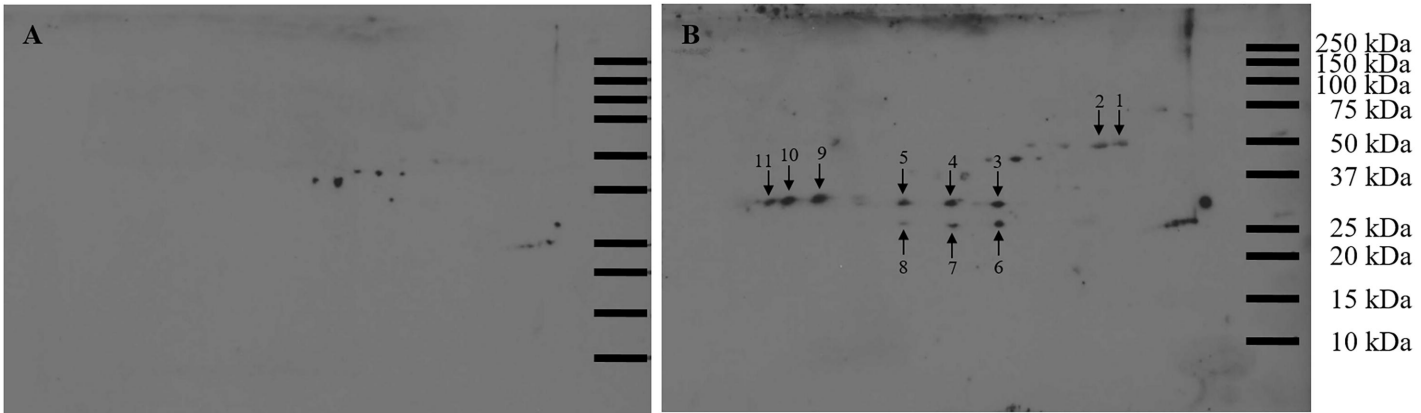
10
pH
3
A
10
pH
3
B
250 kDa
150 kDa
100 kDa
75 kDa
50 kDa
37 kDa
25 kDa
20 kDa
15 kDa
10 kDa
11
10
9
5
4
3
2
1
8
7
6

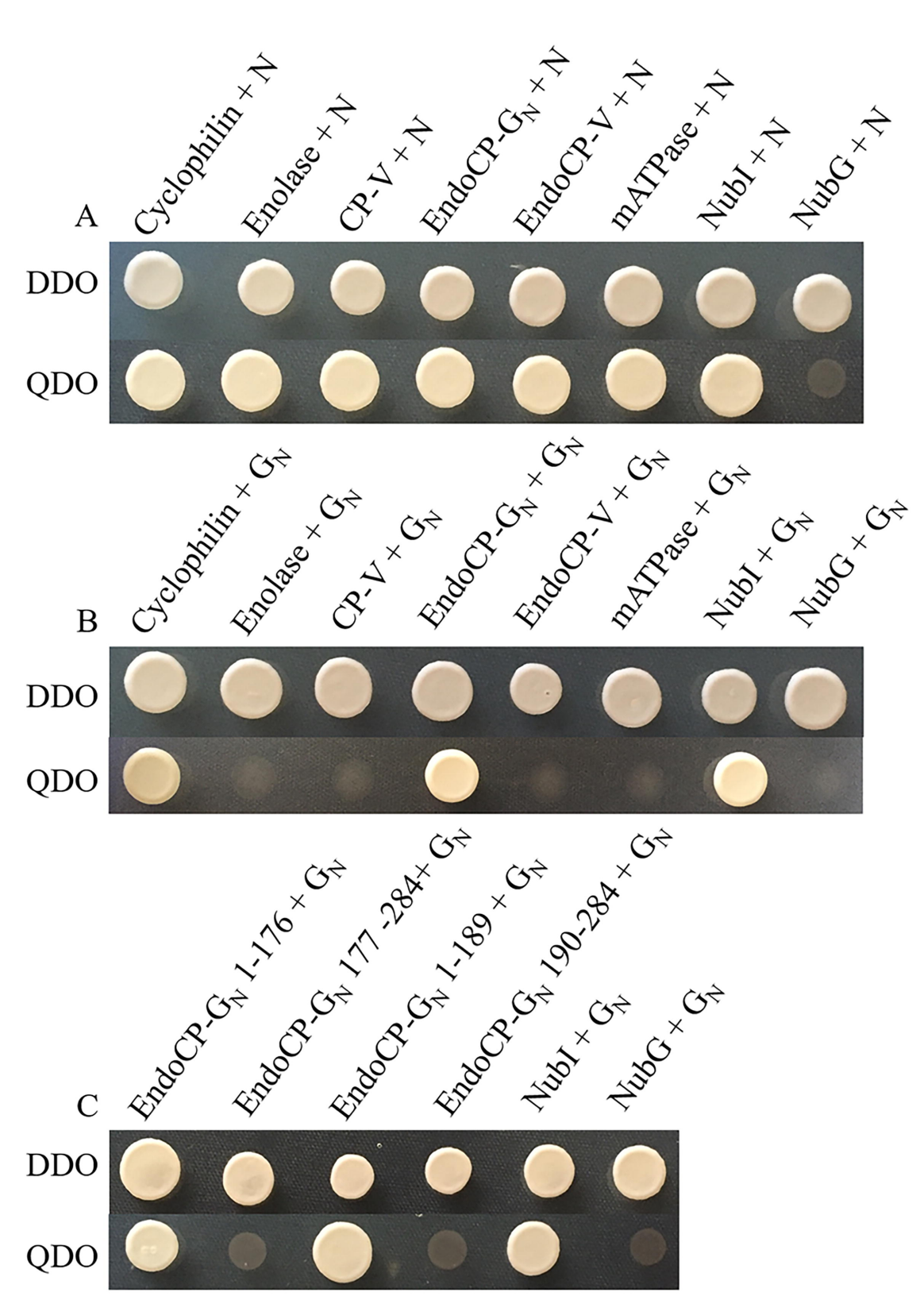
A
Cyclophilin + N
Enolase + N
CP-V + N
EndoCP-GN + N
EndoCP-V + N
mATPase + N
NubI + N
NubG + N
DDO
QDO
B
Cyclophilin + GN
Enolase + GN
CP-V + GN
EndoCP-GN + GN
EndoCP-V + GN
mATPase + GN
NubI + GN
NubG + GN
DDO
QDO
C
EndoCP-GN 1-176 + GN
EndoCP-GN 177 -284+ GN
EndoCP-GN 1-189 + GN
EndoCP-GN 190-284 + GN
NubI + GN
NubG + GN
DDO
QDO

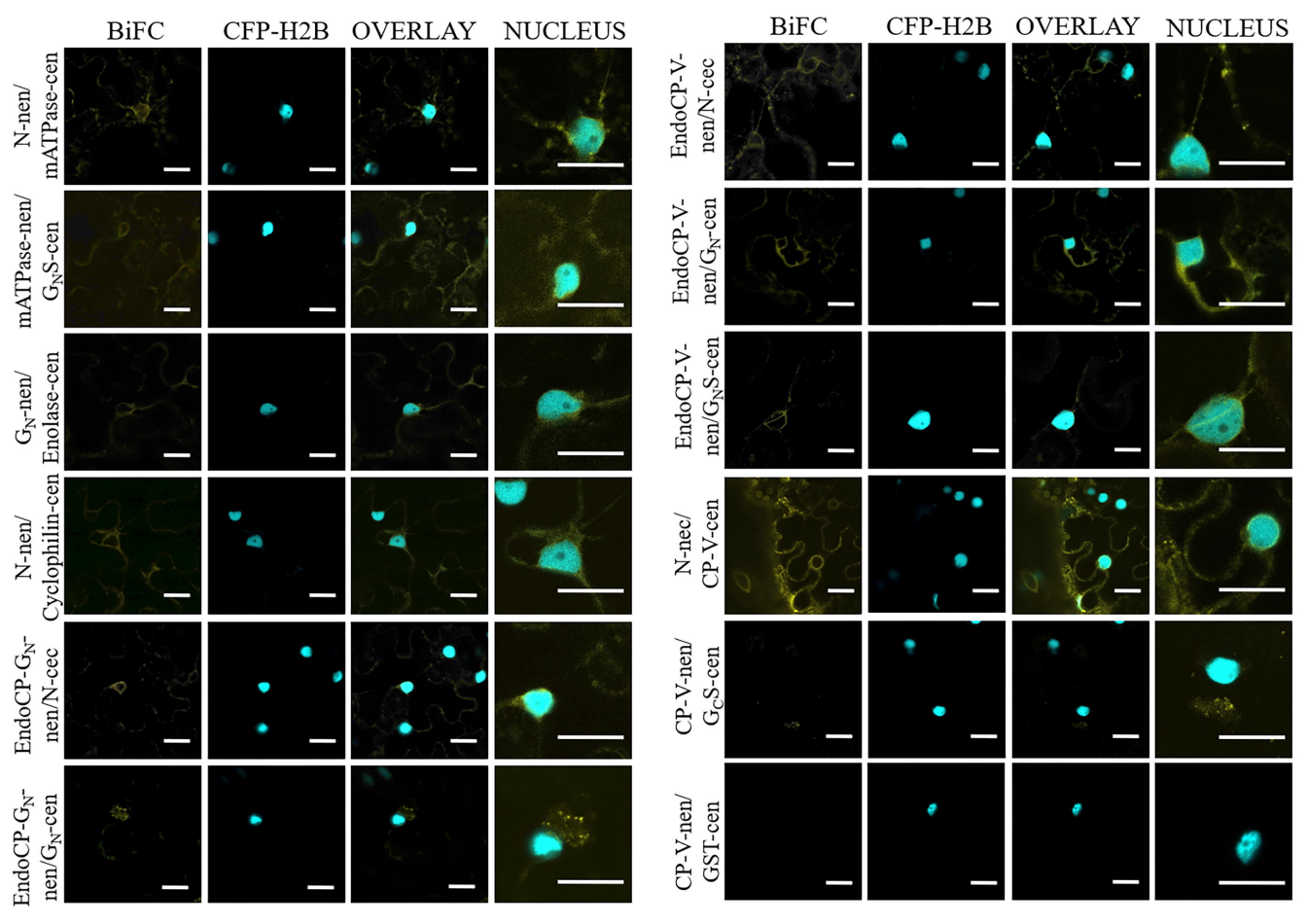
BiFC
CFP-H2B
OVERLAY
NUCLEUS
N-nen/ mATPase-cen
mATPase-nen/ G_NS-cen
G_N-nen/ Enolase-cen
N-nen/ Cyclophilin-cen
EndoCP-G_N-nen/N-cec
EndoCP-G_N-nen/G_N-cen
BiFC
CFP-H2B
OVERLAY
NUCLEUS
EndoCP-V-nen/N-cec
EndoCP-V-nen/G_N-cen
EndoCP-V-nen/G_NS-cen
N-nec/ CP-V-cen
CP-V-nen/ G_CS-cen
CP-V-nen/ GST-cen

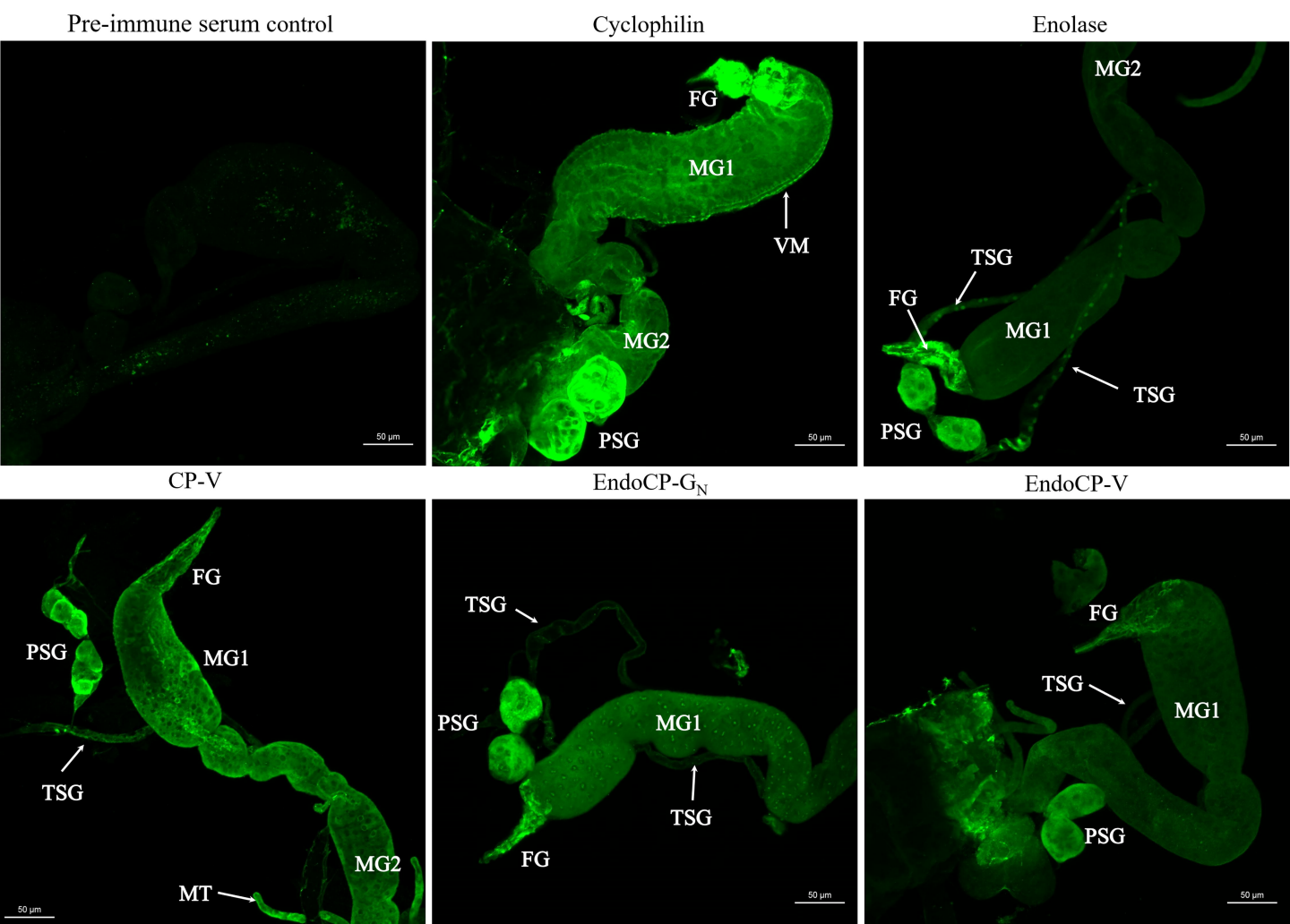
Pre-immune serum control
Cyclophilin
Enolase
FG
MG1
VM
MG2
PSG
TSG
FG
MG1
TSG
PSG
MG2
50 µm
CP-V
EndoCP-G$_N$
EndoCP-V
FG
PSG
MG1
TSG
MT
MG2
TSG
PSG
MG1
TSG
FG
FG
TSG
MG1
PSG

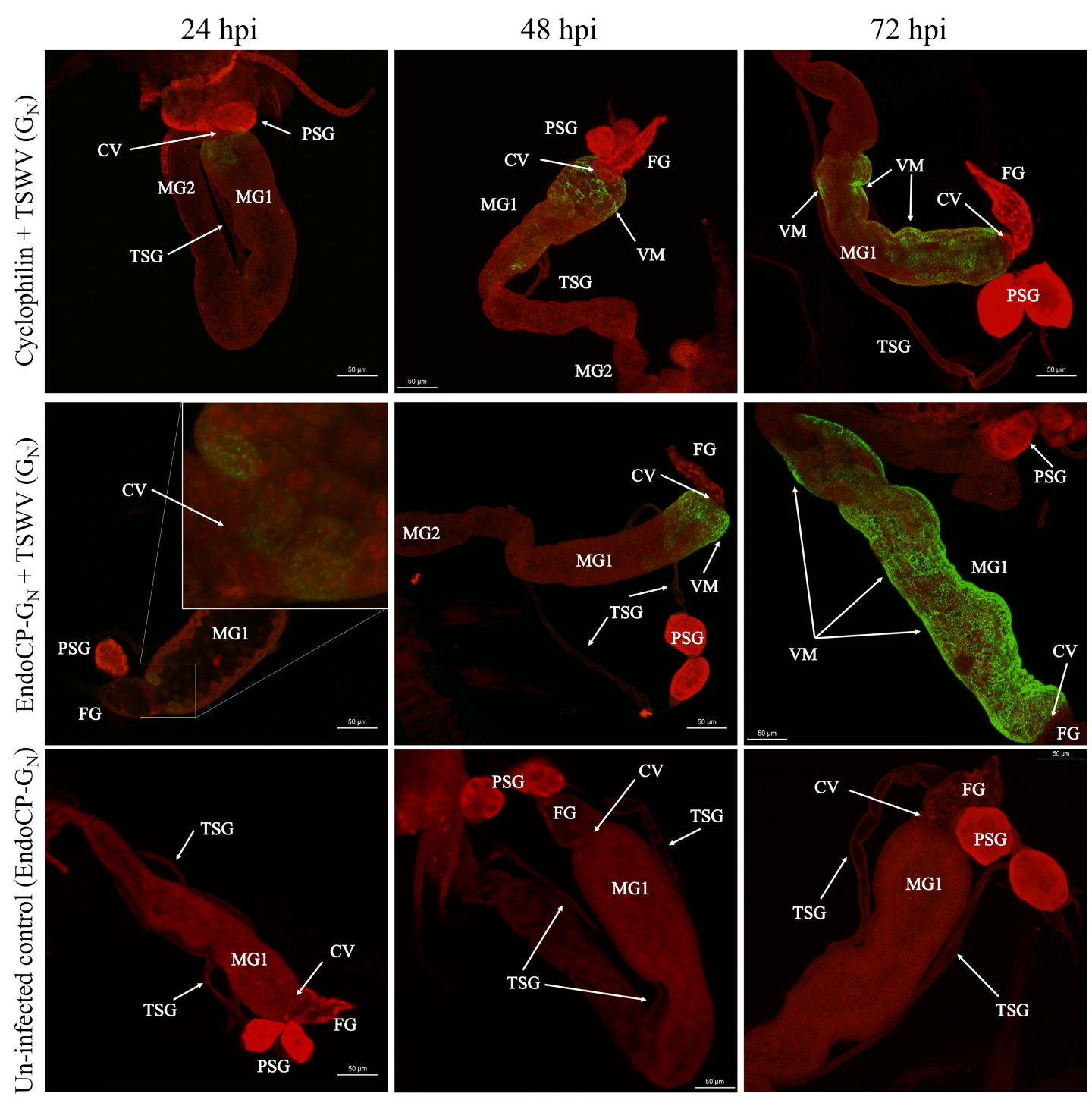
24 hpi
48 hpi
72 hpi
Cyclophilin + TSWV (G_N)
EndoCP-G_N + TSWV (G_N)
Un-infected control (EndoCP-G_N)
CV
PSG
MG2
MG1
TSG
FG
VM
50 µm